Impact of COVID-19 on the Consumer Products and Services Sector of Bursa Malaysia Using Complex Network Analysis

Alyssa April Dellow

Introduction

It is no secret that COVID-19 has turned our lives upside down, may it be economy, education or health wise. The stock market of every country has also been affected by this black swan event, resulting in the changes of its complex relationship that can be studied more conveniently through networks. This report aims to study the networks of the pre, during and post-COVID-19 periods constructed using the stocks in the Consumer Products and Services sector of Bursa Malaysia. This particular sector is chosen as it is one of the biggest sectors in Bursa Malaysia, and it is assumed that many interesting insights can be gained from it. Many kinds of analysis such as visualisations of networks, topological properties, centrality measures and comparisons with values from other network models are done to understand the impact of COVID-19 on the Malaysian stock market. The details of the network, vertices, edges and data set can be found in the subsequent subsections.

Network

In this report, the networks produced are financial networks, which can be used to observe and analyse a stock market's behaviour by portraying the relationship between stocks' closing prices. Financial networks can help to visualise the complex relationship between stocks, more so if the number of stocks is large. The networks consist of stocks from the Consumer Products and Services sector of Bursa Malaysia, which has eight subsectors. The impact of a major event, namely the COVID-19 pandemic, on the Consumer Products and Services sector is studied to gain insights on how one of the biggest sectors in the Malaysian stock market reacts to a crisis. The pre, during and post periods of this major events are utilised to build networks, thus leading to a total of three networks. All the three data sets downloaded from Refinitiv Eikon Datastream for this project are in the form of daily closing prices. The networks are undirected, weighted and do not have multiple edges or loops. A threshold value of mean plus two standard deviations is used to delete edges with weights below this value and above the negative of this value. This is to ensure that the networks are not too dense, which would make it difficult for any interpretations to be made.

The Consumer Products and Services sector networks are represented mathematically by graphs/networks so that analysis can be done easily. Since there are a total of three networks, they are represented mathematically as follows:

$G_1 = (V(G_1), E(G_1))$, where $G_1$is the financial network for the pre-COVID-19 period,

$G_2 = (V(G_2), E(G_2))$, where G_2 is the financial network for the during COVID-19 period, and

$G_3 = (V(G_3), E(G_3))$, where G_3 is the financial network for the post-COVID-19 period.

Here $V(G_i)$ represents a set of vertices and $E(G_i)$ represents a set of edges with $i = 1,2,3$.

Vertices

The vertices for these networks are the stocks of the Consumer Products and Services sector. Note that originally, 168 stocks were downloaded from Refinitiv Eikon Datastream. However, only 162 stocks are utilised as the vertices of all three networks. The reason for this is explained in more detail in the Data subsection. For deeper analysis purposes, the vertices of the networks are coloured according to their respective subsectors. This enables any clustering insights to be made.

For all three networks, the set of vertices for G_i can be represented by $V(G_i)$, where $i = 1,2,3$.

$V(G_i) = \{v \mid v \text{ is a stock in the Consumer Products and Services sector}\}$

$V(G_i)$ = {ABLE, ADVA, AEOM, AFCB, AFHB, AIRX, AJIN, AMWA, ARTW, ASIA, ATLA, AVIL, BATO, BERA, BESH, BJFO, BLAD, BONI, CABC, CAEY, CAPI, CBMS, CCKH, CCLD, CETH, CIHB, CITR, COWH, CRSM, CSCB, CWGH, DBMS, DELM, DRBM, EMIC, ENGH, ERHB, ESAN, ESTH, FCWH, FIAM, FIHB, FPIB, FRAS, GENM, GENT, GLOA, GNCH, GRAN, GRYB, HBGL, HEIN, HLIB, HOME, HSIB, HSON, HWAT, ICOI, IMPI, IQGH, JADI, JAYC, JERA, KARE, KHEE, KHIN, KMDA, KSTM, KWNF, LAYH, LHEN, LHTM, LMHS, LOTU, LTKM, MAGM, MATE, MBMR, MESB, METB, MFMS, MILU, MIND, MITC, MRHB, MSMH, MUIB, MYNE, NESM, NHFH, NHSN, NICH, NTPM, OCBB, OCEA, OFIH, OLYM, ONEG, ONLY, OTLS, PAOS, PCCS, PDNI, PELK, PENS, PEPT, PERM, PERT, PETR, PGKN, PGON, PHUA, PMCS, PMJU, PMMY, POHK, POWE, PRGH, PRKN, PWFC, PXUS, QRES, RENE, REXI, RGBI, RHOG, RHON, SALU, SAND, SAUD, SEDU, SEVE, SGNA,

SHGM, SHHR, SIME, SINA, SINM, SKOU, SOIL, SPOR, SPTZ, SWSB, SYFR, TAFI, TGLB, TGPB, THEA, TMEI, TNCS, TPCP, TSCP, TSHB, UMWS, UPAB, WATC, WEGM, WGZH, XIDE, XLHO, YGON, ZHCO}

Each four-letter element in $V(G_i)$ represents the ticker for a respective stock.

The number of vertices in G_i, also known as the order of G_i is:

$N(G_i) = 162$, that is all 162 stocks.

Edges

The edges for these networks are the correlations between stocks of the Consumer Products and Services sector based on their daily closing prices. For example, the correlation among two stocks, namely stock $p \in V(G_i)$ and stock $q \in V(G_i)$, based on their daily closing prices is described by the edge, $e = \langle p, q \rangle \; or \; e_{pq}$, which associates the two stocks p and q. These closing price correlations between stocks can represent the weight of the edges where a pair of stocks with stronger correlation have a thicker edge between them. Thus, we have weighted edges where every $e \in E(G_i)$ has its own unique weight w_{pq}. Besides that, the networks built in this report include negative weights as well to enable any interesting discoveries. The edges are in blue if the pair of stocks have a positive correlation and are in red otherwise.

For all three networks, the set of edges for G_i can be represented by $E(G_i)$, where $i = 1,2,3$.

$E(G_i) = \{e \mid e \; is \; the \; correlation \; between \; two \; adjacent \; stocks \; based \; on \; their \; daily \; closing \; prices\}$

Before removing edges based on the threshold network approach to reduce the density of the networks, all 162 stocks were adjacent to one another. Therefore, each of the three networks had the maximum number of edges possible, L_{max}, as they were complete networks.

$$L_{max} = \binom{N(G_i)}{2} = \binom{162}{2} = 13041$$

The number of edges in G_i, also known as the size of G_i, after the removal of edges is stated in the Threshold Networks subsection based on their respective periods.

Data

This project utilises the stocks from the Consumer Products and Services sector of Bursa Malaysia to construct networks. The Consumer Products and Services sector is one of the sectors contained in the Bursa Malaysia Sectorial Index Series, which tracks the performance of all stocks listed on the Main Market. This sector has eight subsectors, namely, Agricultural Products, Automotive, Consumer Services, Food and Beverages, Household Goods, Personal Goods, Retailers, and Travel, Leisure and Hospitality. Each stock in the network plots will be coloured according to their respective subsectors. Data is extracted in the form of daily closing prices from Refinitiv Eikon Datastream in Excel by referring to the constituent list in Refinitiv Eikon. Altogether, data from three time intervals are extracted as shown in Table 1. Note that the length of the pre and post-COVID-19 periods are determined by the length of time chosen for the during period as to unify each interval's length. For analysis purposes, the intervals are taken from the first day of the month to the last day of the month to ensure that data is collected from complete months.

Table 1. [Pre, during and post-COVID-19 period intervals]

Major Event Period	Interval	Reason For Interval Chosen	Number Of Trading Days
Pre-COVID-19	1 September 2018 to 30 November 2019	The start date is chosen as such because the first cases of COVID-19 were reported in December 2019. The end date is set as 28 February 2021 due to the fact that the immunisation programme started in Malaysia in February 2021.	325
During COVID-19	1 December 2019 to 28 February 2021		325
Post-COVID-19	1 March 2021 to 31 May 2022		327

The number of stocks utilised are less than the original number of stocks downloaded due to data availability as some stocks were only listed on the Main Market after the intervals specified. Companies that were listed after the start date of the pre-COVID-19 period, are not included in the analysis, leading us to have 162 stocks. As of 30 October 2022, there are 168 stocks listed in the Consumer Products and Services sector. All 6 stocks removed from the analysis are listed in Table 2.

Table 2. [Listing dates for stocks that were removed from analysis]

No.	Company Name	Listing Date	Subsector
1	Farm Fresh	22 March 2022	Food & Beverages
2	Innature	20 February 2020	Personal Goods
3	Leong Hup International	16 May 2019	Agricultural Products
4	MR DIY Group M Berhad	26 October 2020	Retailers
5	Senheng New Retail	25 January 2022	Retailers
6	Yenher Holdings	15 July 2021	Agricultural Product

Network analysis is carried out on all three intervals of data to study and compare the impacts of the COVID-19 pandemic on the Consumer Products and Services sector of Bursa Malaysia. Changes on each network over time are observed to draw conclusions. All analyses are carried out in RStudio version 4.2.1, with a special emphasis on the igraph package.

Threshold Networks

In the interest of assessing the impact of COVID-19 on the Consumer Products and Services sector of the Malaysian stock market, threshold networks for the pre, during and post COVID-19 periods are constructed to enable comparisons over time. The procedures involved in constructing threshold networks are listed in order below:

a) Rate of Return

Compute the logarithmic returns of stocks by defining $P_i(t)$ as the closing price for stock $i \in V(G)$ on day t, and $r_i(t)$ as the logarithmic return for stock i on day t.

$$r_i(t) = ln\left[\frac{P_i(t)}{P_i(t-1)}\right]$$

b) Correlation Matrix

For a network with N stocks, an $N \times N$ Pearson correlation matrix can be computed to attain the correlations between all pairs of stocks based on their daily closing prices. The Pearson correlation coefficient among any two stocks, $i \in V(G)$ and $j \in V(G)$, from the matrix, is calculated as follows (Mantegna 1999):

$$C_{ij} = \frac{\langle r_i r_j \rangle - \langle r_i \rangle \langle r_j \rangle}{\sqrt{(\langle r_i^2 \rangle - \langle r_i \rangle^2)(\langle r_j^2 \rangle - \langle r_j \rangle^2)}}$$

where C_{ij} is the correlation between the two stocks mentioned or in other words, their edge weight, and <…> denotes the average of its content. Having N stocks, an $N \times N$ dimensioned cross-correlation characterised by L_{max} correlation coefficients completely, with values $-1 \leq C_{ij} \leq 1$, is constructed. The values of C_{ij} indicate the strength and direction of the linear relationship between stocks i and j as can be seen below:

$$C_{ij} = \begin{cases} 1 & perfect\ positive\ correlation\ between\ stock\ i\ and\ stock\ j \\ 0 & no\ correlation\ between\ stock\ i\ and\ stock\ j \\ -1 & perfect\ negative\ correlation\ between\ stock\ i\ and\ stock\ j \end{cases}$$

c) Set the threshold value

All three threshold networks in this report are generated based on a threshold value, θ, of mean plus two standard deviations of the correlation matrix. Based on a study by Silver and Dunlap (Silver et al. 1987), the mean of correlation coefficients tends to underestimate the population correlation. But even so, the Fisher's *z* transformation can almost completely fix this problem. The next step is to figure out the average of the *z* values, which on the other hand tends to overestimate the population value even though the distribution of *z* is approximately normal. Instead of just taking the average of the correlation coefficients, it would be less biased to use the inverse Fisher transform to turn the average of *z* back into a correlation coefficient. This final value of the correlation coefficient is implemented as the mean of the correlation matrix, $\bar{C}$. In light of this, the threshold value for each network is set to $\bar{C} + 2\sigma$. The following formula is for the Fisher's *z* transformation(Fisher 1934):

$$z = 0.5 \ln\left[\frac{1 + C}{1 - C}\right]$$

where *z* is the Fisher's *z* and C is the cross-correlation coefficient. The formula below is the inverse Fisher transform:

$$\bar{C} = \frac{(e^{2z} - 1)}{(e^{2z} + 1)}$$

d) Remove edges

The threshold values, θ, that are statistically computed based on the respective correlation coefficients for each period, satisfies $-1 \leq \theta \leq 1$. When $C_{ij} > \theta$ or $C_{ij} < -\theta$, an undirected edge develops between stocks i and j. Hence, edges with weights below the threshold value set and above the negative of this value are deleted from the network. Since every period has its own unique threshold value, the threshold networks generated each have the same number of vertices but vastly different numbers of edges.

e) Create *igraph* objects after removing the edges and plot the threshold networks.

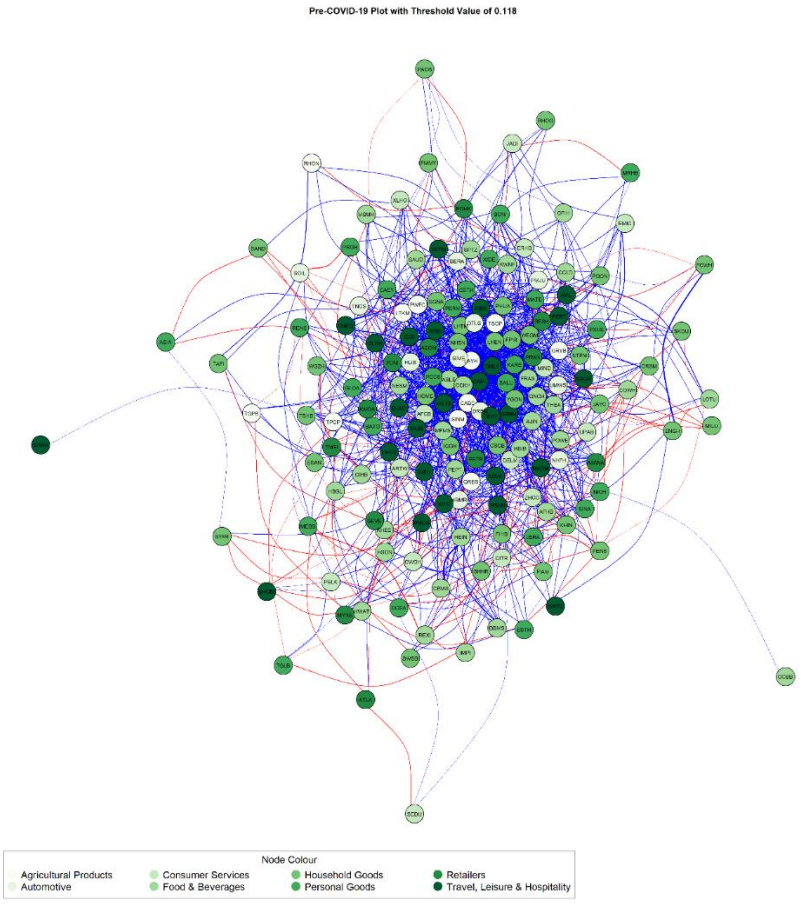

Figure 1. [Threshold network of the pre-COVID-19 period constructed using a threshold value of 0.118]

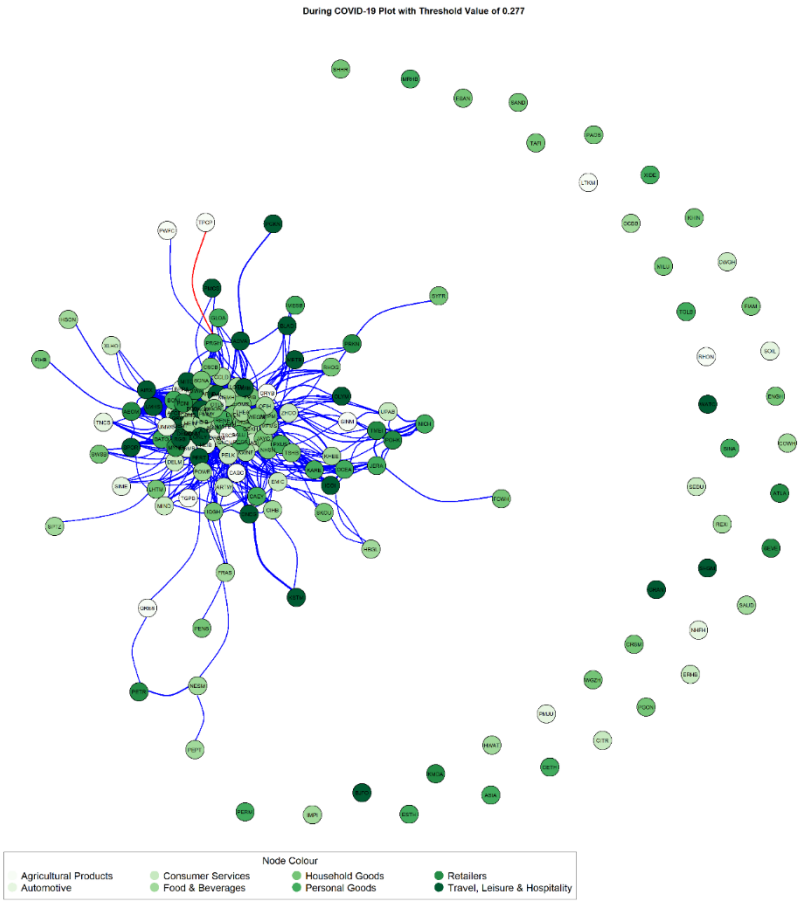

Figure 2. [Threshold network of the during COVID-19 period constructed using a threshold value of 0.277]

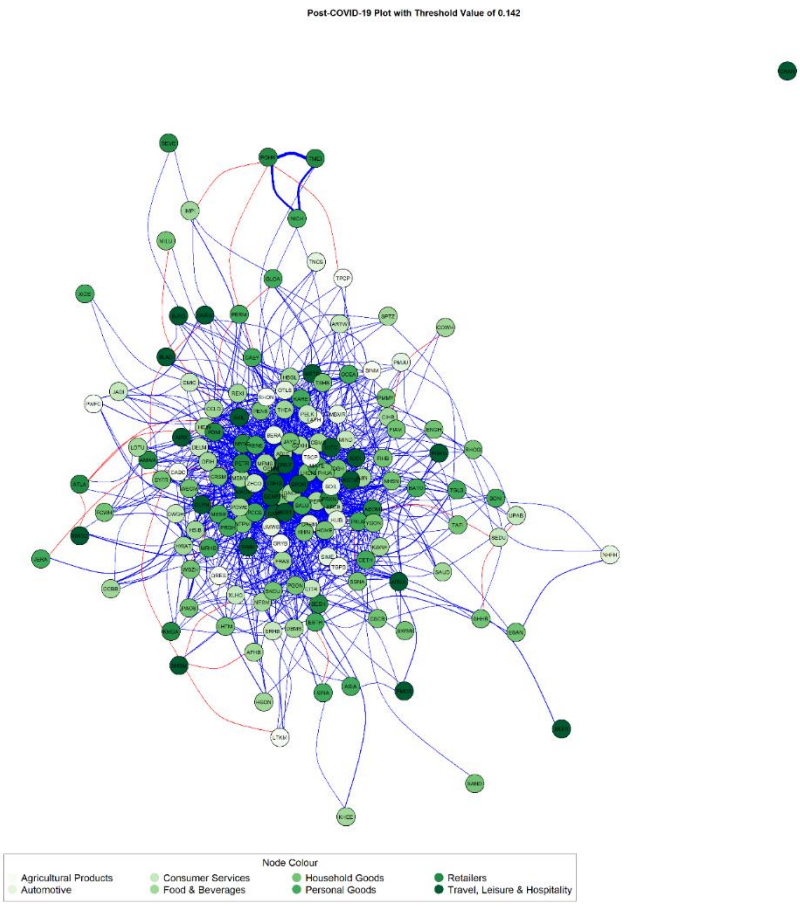

Figure 3. [Threshold network of the post-COVID-19 period constructed using a threshold value of 0.142]

Many observations can be made by carefully looking at Figure 1, Figure 2 and Figure 3. All three networks appear quite dense since there are 162 stocks in the Consumer Products and Services sector of Bursa Malaysia. At a glance, there is a visible change in the network structure of the during COVID-19 period as compared to the pre and post periods. First of all, in the pre-COVID-19 period, the whole network is connected and not a single isolated stock can be seen. However, in the during period, 42 stocks are disconnected from the largest component, leaving only 120 stocks in the giant component. These 42 components of size one are called singleton vertices. The singleton vertices will not be easily influenced by negative spillovers from other stocks, making them a safe option for risk averse investors who would like to build a 1ess risky portfolio during the crisis. Nevertheless, it also depends on the stocks' performance as they cannot even be positively influenced by other stocks. All the singleton vertices, except for Grand Central Enterprises (GRAN) from the Travel, Leisure and Hospitality subsector, have rejoined the giant

component in the post period. GRAN remaining on the periphery of the network indicates that it might have been heavily impacted by the pandemic, which makes sense since this company is in the hotel business. Any businesses involved in tourism were heavily affected by the pandemic following lockdowns and travel bans, making it a long way to recovery.

Next, view how the number of negative correlations between pairs of stocks abruptly decreases in the during period. This shows a change in the direction of correlation for many stocks, where they move in the same direction during the strike of events that bring about high volatility. In the pre period, it was much more common for stock prices to move in the opposite direction. It would be much easier for investors who want to diversify their portfolio in the pre period, as many more stocks have prices that move in opposite directions. A fall in the price of one stock would indicate a rise in the other. TPC Plus (TPCP) from the Agricultural Products sector and PRG Holdings from the Personal Goods subsector are the only pair of vertices that have a negative correlation in the during period. Lastly, there is no clear indication of clustering according to subsectors as the stocks seem to be scattered. But it is worth noting that quite many stocks from the Travel, Leisure and Hospitality sector seem to be in the centre of the network in the post period. In the Centrality Measures section of this report, it is found that this sector conquers the post period.

In addition, the thickness of the edges visibly increase in the during period, proving that the stocks are more closely correlated and interconnected, as can also be seen by how the stocks huddle close together, overlapping one another in the network plot. Even with the highest threshold value of 0.277 in the during period, the network still has the highest density of 0.118 as can be seen in Table 3. The study of Memon (2022) also shows similar results, indicating herd behaviour in the stock network caused by the uncertainty of the crisis. The clusters in the pre and post period are relatively weak compared to that of the during period. Another fascinating discovery that can be made is that in the post period, Poh Kong Holdings (POHK), Tomei Consolidated Berhad (TMEI) and Niche Capital Emas Holdings (NICH), are all adjacent with one another through evidently thick positive edges. These three companies are all involved in the jewelry business, and the influence they have on one another is powerful.

Minimum Spanning Tree (MST)

Alternatively, a Minimum Spanning Tree (MST) can be constructed for each period as MST is one of the famous approaches to study the relationship between stocks and the complex developments of their financial networks. A spanning tree of a graph, G, is a subgraph such that all the vertices in the subgraph are connected, acyclic and includes every single $i \in V(G)$. An MST on the other is a spanning tree with the minimum possible sum of edge weights. Kruskal's algorithm and Prim's algorithm are used by many researchers to extract the MST, but for this report, Kruskal's algorithm is employed.

To construct MSTs, the first and second steps are similar to steps (a) and (b) in the Threshold Network section. The subsequent steps are listed down below:

c) Distance Matrix

According to Mantegna (Mantegna, 1999), the correlation coefficient, C_{ij}, between two stocks cannot be used as a measure of their distance since it does not satisfy the three axioms that constitute a Euclidean metric. These three axioms are:

- $d_{ij} = 0$ if and only if $i = j$
- $d_{ij} = d_{ji}$
- $d_{ij} \leq d_{ik} + d_{kj}$

Also note that d_{ij} conforms to the following property:

$$d_{ij} = \begin{cases} 0 \; if \; the \; prices \; of \; stock \; i \; and \; j \; are \; perfectly \; correlated \\ 2 \; if \; the \; prices \; of \; stock \; i \; and \; j \; are \; inversely \; correlated \end{cases}$$

Nevertheless, a distance matrix, $D = d_{ij}$, can be constructed from the correlation matrix by transforming C_{ij} into distance as stated below:

$$d_{ij} = \sqrt{2(1 - C_{ij})}$$

d) Kruskal's Algorithm

The construction of MSTs from the distance matrix in step (c) is achieved through Kruskal's algorithm as recommended by Kruskal (Kruskal 1956). The first step to build

MSTs using Kruskal's algorithm is to sort all the distances in ascending order. Then, select the shortest edge in the network, followed by the next shortest edge which does not create a cycle, since MSTs are acyclic. This step is repeated until all the N vertices have been connected. The completed MST will consist of N vertices with $N - 1$ edges.

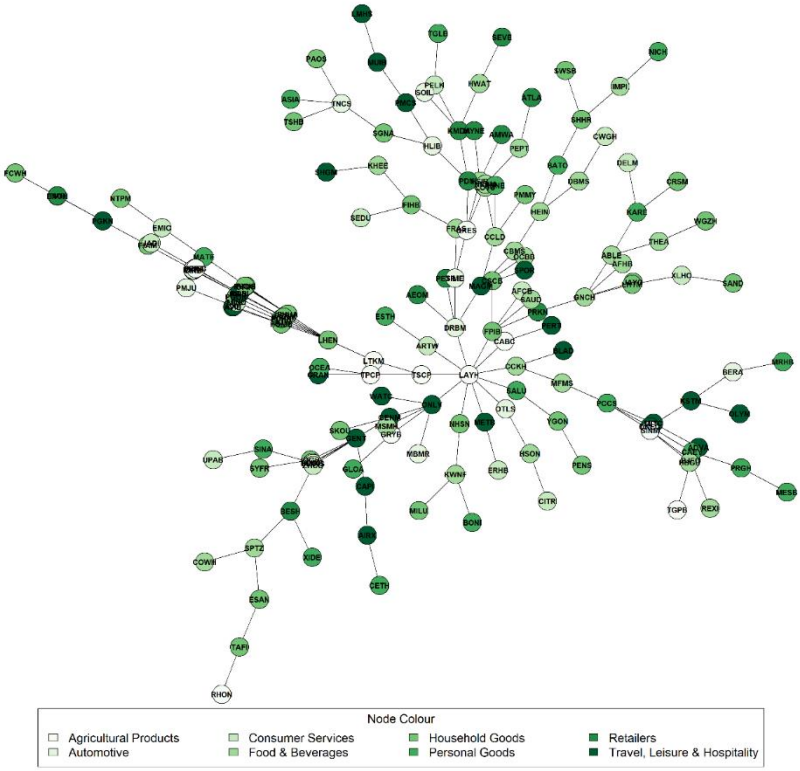

Figure 4. [Minimum Spanning Tree of the pre-COVID-19 period]

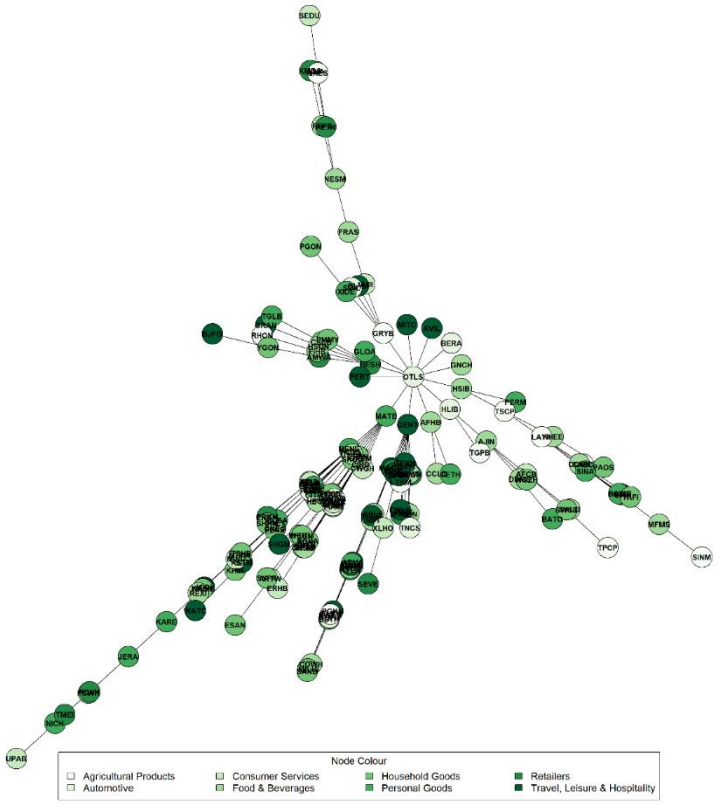

Figure 5. [Minimum Spanning Tree of the during COVID-19 period]

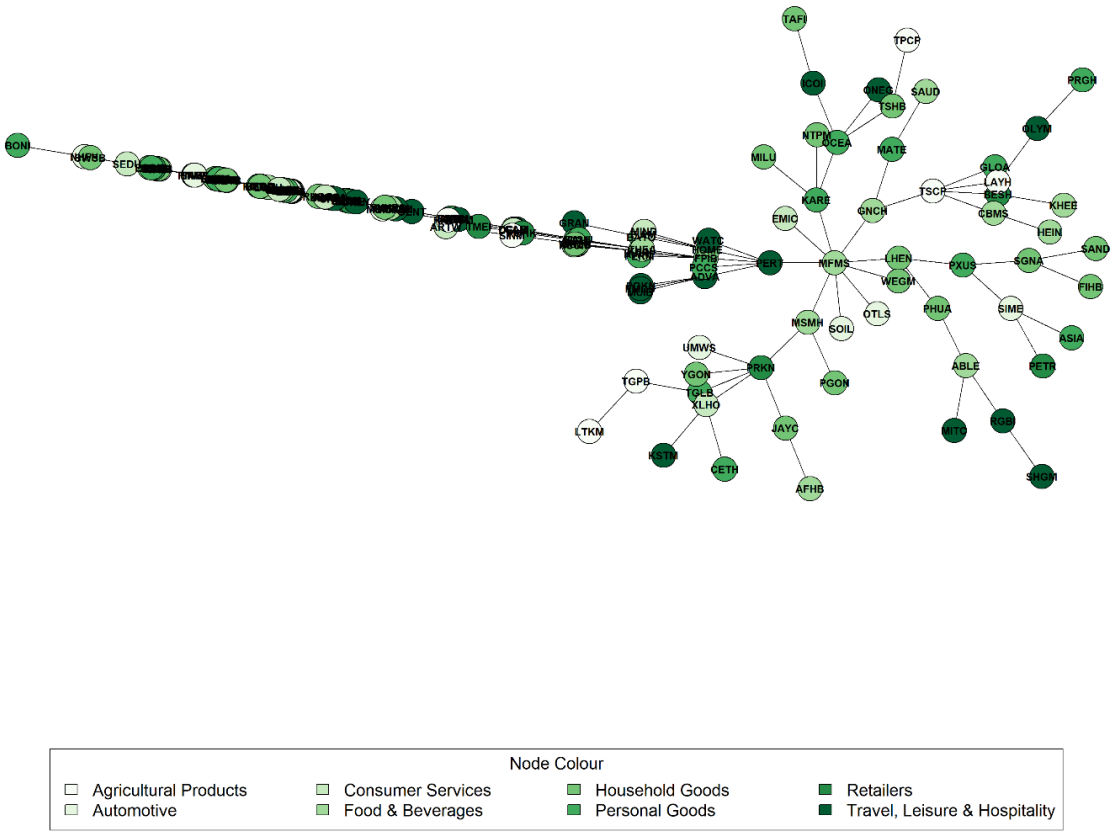

Figure 6. [Minimum Spanning Tree of the post-COVID-19 period]

Based on Figure 4, Figure 5 and Figure 6, the MSTs of the pre, during and post-COVID-19 periods can be analysed. In the pre-COVID-19 period, Lay Hong (LAYH), an agricultural products company, is in the centre of the whole network with 11 direct connections. The next cluster is led by Only World Group Holdings (ONLY) from the Travel, Leisure and Hospitality sector with 5 adjacent companies. DRB-Hicom (DRBM) and Formosa Prosonic (FPIB) from the Automotive and Household Goods subsectors on the other hand, lead their own clusters with four connections each. ONLY, DRBM and FPIB are all first neighbours of LAYH. These dominant stocks directly connect with stocks from various subsectors, not only those from their own subsector. The interrelationship between stocks from different subsectors can also be seen in the study of Yee et al. (2018) on the top 100 stocks in Bursa Malaysia.

For the during COVID-19 MST, the hubs of the network changes completely. Right in the centre of the network is Oriental Holdings (OTLS) from the Automotive subsector with 13 links to other

stocks. Besides that, Genting (GENT) from the Travel, Leisure and Hospitality sector, and Magni-Technology Industries (MATE) from the Personal Goods sector, also have a significant number of connections, leading their very own clusters. None of the earlier hubs have maintained their positions during the crisis, indicating the hard impact caused by the pandemic on central stocks and the emergence of new key players.

Moving on to the post-COVID-19 period, the number of vertices that are adjacent to a hub have decreased, similar to the findings of Bahaludin et al. (Bahaludin et al. 2019) on the top 100 companies in Bursa Malaysia. Once again, the stocks that act as hubs change to Malayan Flour Mills (MFMS) with 9 connections and its first neighbour, Pertama Digital (PERT), with 5 connections. The stocks are from the Food and Beverages, and Personal Goods subsectors respectively. Most of the mentioned hubs such as LAYH, ONLY, DRBM, FPIB, OTLS, MATE and MFMS, also appear in the top 5 for certain centrality measures (Table 4), according to their respective periods. This only solidifies their importance in the Consumer Products and Services sector, and they must be focused on when regulating policies to boost the stock market. Risk-takers should invest in more dominant stocks as they could give extreme returns in either end.

Descriptives

In order to view changes in the network structure over each period, some network statistics are displayed in Table 3. These statistics also aid as additional information to readers who wish to understand the situation during a crisis more clearly.

Density here represents edge density, in which when a pair of vertices are picked at random, the probability that they are connected is equivalent to the density, p. It is the number of edges observed in a network over the maximum number of edges possible.

$$p = \frac{L}{(N(N-1))/2}$$

The average degree of an undirected network, $\langle k \rangle$, is simply the average over the degree values of every vertex in the network.

$$\langle k \rangle = \frac{1}{N} \sum_{i=1}^{N} d_i$$

where d_i is the degree of $i \in V(G)$.

Table 3. [Network statistics of each of the three stock networks]

Interval	Threshold Value	Edges	Density	Average Degree
Pre	0.118	1464	0.112	18.074
During	0.277	1544	0.118	19.062
Post	0.142	1347	0.103	16.630

From Table 3, it is clear that the threshold value during the COVID-19 period is around double of the pre and post periods. This indicates higher mean and standard deviation values during a crisis. a higher mean correlation value could mean that the stocks belong to tighter groups, moving in homogenous directions. The number of edges should coincide with the density of a network. As expected, the density in the during crisis period is the highest, at a value of 0.118, similar to the finding of another study regarding the Hong Kong stock market (So et al. 2021). Higher density values lead us to believe that the network experiences an increase in interconnectedness, which may lead to a more vulnerable market. This is due to the contagion spreading mechanism, where any impact is amplified because of the stocks' close relations.

In accordance with the findings of a study regarding the Chinese stock market (Xia et al. 2018), the average degree shows the highest value of 19.062 during the crisis. This simply means that the cross-correlations among stocks are strengthened during turbulent times. The average degree value however drops quite a lot in the post-COVID-19 period, showing weaker cross-correlations than the other two periods.

It can be said that the COVID-19 pandemic has added fluctuations to some extent to the Malaysian stock market in the Consumer Products and Services sector. During a crisis, mean and standard deviations of the correlations, number of edges, density and average degree rise, all signs of higher correlation among stocks. Markets tend to be more volatile, which is not unusual given the circumstances of the negative external shocks brought forth by the black swan event. It is shown

by Sandoval and Franca (2012) that markets frequently act in unison during severe market crashes. Without doubt, the outbreak has certainly increased the systemic risk of the Malaysian stock market.

Centrality Measures

Centrality measures in undirected networks are used to identify stocks that occupy an influential position, based on their direct or indirect adjacency with other stocks (Luke, 2015). In this section, we focus on characterization by cohesiveness where we compute degree, eigenvector, closeness and betweenness centralities of the stocks. Each centrality has their own definitions and algorithms, leading to a variety of results depending on what type of centrality needs to be measured.

Start with the most conceptually simple centrality measure, that is degree centrality. This centrality measures importance based on the number of edges connected to a vertex. The degree of each vertex can be ranked, where more influential vertices have more direct neighbours than vertices with fewer direct neighbours. This centrality captures only a local measure of importance, where all connections are assumed to be equal.

$$C_D(i) = d_i$$

A natural generalisation of degree centrality to increase the importance of vertices adjacent to other high-degree vertices is portrayed by eigenvector centrality. Eigenvector centrality determines influential vertices in terms of the number direct and indirect neighbours a vertex has, besides rendering all vertices with unequal importance, as some neighbours could contribute more influence than others. Eigenvector centrality can be calculated based on the adjacency matrix of a network as follows:

$$C_E(i) = \frac{1}{\lambda}\sum_{j=1}^{N} A_{ij}x_j$$

where λ is the largest eigenvalue of the adjacency matrix A, A_{ij} is an element of A and x_j is the leading eigenvector of stock j.

The prominence of stocks within financial networks can also be measured using closeness centrality. Closeness centrality is the sum of the length of the shortest paths from a vertex to all other vertices, where central vertices are situated closer to other vertices. This centrality is important to study the effects of a crisis in a network as spillovers can spread quickly if vertices are situated in close proximity to each other. Mathematically, the closeness centrality of $i \in V(G)$ can be expressed in the following equation:

$$C_C(i) = \left[\sum_{j=1}^{N} d(i,j)\right]^{-1}$$

where $d(i,j)$ is the length of the shortest path between stock i and stock j.

Lastly, is betweenness centrality that measures the extent to which a vertex lies on paths between other vertices. Vertices that are considered influential according to betweenness centrality have the ability to control information flow in a network since they are similar to brokers. Without these high betweenness vertices, communication between other vertices in the network will be significantly disrupted. This centrality is quite different from the other three centrality measures in that it captures how much a vertex falls between others, in contrast to measuring how well connected a vertex is. Having said that, vertices can possess high betweenness values but low degree, eigenvector or closeness values. The expression below represents betweenness centrality in mathematical terms.

$$C_B(i) = \frac{2}{(N-1)(N-2)} \sum_{p<q}^{N} \frac{g_{pq}(i)}{g_{pq}}, i \neq q \neq p$$

with $g_{pq}(i)$ being the number of shortest paths connecting stock p and q that pass-through stock i, while g_{pq} is the total number of shortest paths between stock p and q. This equation involves normalisation, where the betweenness values are normalised by the number of ordered or unordered vertex pairs in the network. This enables betweenness values to fall between 0 and 1 so that networks can conveniently be compared with one another.

Table 4. [Top 5 stocks with the highest centrality measures, namely degree, eigenvector, closeness and betweenness centralities, for each period]

No.	Pre		During		Post	
Degree Centrality						
1	DRB-Hicom (DRBM)	63.000	Beshom Holdings (BESH)	70.000	Genting Malaysia (GENM)	64.000
2	Lay Hong (LAYH)	56.000	Magni-Technology Industries (MATE)	70.000	Genting (GENT)	61.000
3	Genting (GENT)	51.000	Oriental Holdings (OTLS)	69.000	Malayan Flour Mills (MFMS)	53.000
4	Capital A (CAPI)	49.000	DRB-Hicom (DRBM)	67.000	Only World Group Holdings (ONLY)	53.000
5	Only World Group Holdings (ONLY)	49.000	Guan Chong (GNCH)	67.000	Formosa Prosonic (FPIB)	50.000
Eigenvector Centrality						
1	Lay Hong (LAYH)	1.000	Oriental Holdings (OTLS)	1.000	Genting Malaysia (GENM)	1.000
2	DRB-Hicom (DRBM)	0.922	Magni-Technology Industries (MATE)	0.969	Genting (GENT)	0.991
3	Only World Group Holdings (ONLY)	0.799	Beshom Holdings (BESH)	0.937	Only World Group Holdings (ONLY)	0.755
4	Genting (GENT)	0.791	Teo Seng Capital (TSCP)	0.910	Capital A (CAPI)	0.671
5	Formosa Prosonic (FPIB)	0.704	DRB-Hicom (DRBM)	0.890	Malayan Flour Mills (MFMS)	0.617
Closeness Centrality						
1	Able Global (ABLE)	0.004	DRB-Hicom (DRBM)	0.006	Genting Malaysia (GENM)	0.004
2	Capital A (CAPI)	0.004	Guan Chong (GNCH)	0.006	Genting (GENT)	0.004
3	DRB-Hicom (DRBM)	0.004	Magni-Technology Industries (MATE)	0.006	Malayan Flour Mills (MFMS)	0.004
4	Genting (GENT)	0.004	Oriental Holdings (OTLS)	0.006	Only World Group Holdings (ONLY)	0.004
5	Lay Hong (LAYH)	0.004	Reneuco (RENE)	0.006	Able Global (ABLE)	0.003
Betweenness Centrality						
1	DRB-Hicom (DRBM)	0.044	Guan Chong (GNCH)	0.036	Genting (GENT)	0.050
2	Genting (GENT)	0.037	Beshom Holdings (BESH)	0.032	Malayan Flour Mills (MFMS)	0.045
3	Able Global (ABLE)	0.036	DRB-Hicom (DRBM)	0.027	Genting Malaysia (GENM)	0.042
4	Only World Group Holdings (ONLY)	0.036	CCK Consolidated Holdings (CCKH)	0.023	Only World Group Holdings (ONLY)	0.039
5	Capital A (CAPI)	0.032	Magni-Technology Industries (MATE)	0.023	Formosa Prosonic (FPIB)	0.032

From a glance at Table 4, the Consumer Products and Services sector does not have much resilience against the pandemic as it seems to be deeply affected. The most influential stocks for each period based on their respective centrality measures vary, appearing and disappearing from the top 5 without a distinguishable pattern. An initial observation about the most influential subsector for each period can be made by looking at the top 5 stocks. It is observed that the Travel, Leisure and Hospitality subsector conquers the pre and post-COVID-19 period, more so in the post period. This is because stocks from this subsector appear the most times in these two periods for all centrality measures as compared to stocks from any other subsector. However, in the during crisis period, stocks from the Travel, Leisure and Hospitality subsector do not even appear once, indicating how badly this subsector was hit by the pandemic. Travel bans, movement restrictions and lockdowns implemented by the Malaysian government during the crisis period to curb the

spread of the virus might have been the biggest contributing factor leading to massive losses in the traveling, leisure and hospitality industries. This subsector could not play a key role during the crisis period due to its huge loss in business.

In the during crisis period, stocks from the Automotive subsector occur most frequently. This makes it the most important subsector during a crisis, and thus must be paid close attention to by authorities to enable the proper implementation of policies. Moving on to the post period, all the first ranking stocks are from the Travel, Leisure and Hospitality subsector. This means that this subsector managed to bounce back from its fall during the pandemic once movement and travel was allowed again. People would spend money on travel and leisure as movement restrictions are lifted, especially with all the promotions to attract customers, which enables this subsector to thrive. This subsector certainly is the heart of the Consumer Products and Services sector during normal periods of time but is hugely affected and takes a big downfall during a crisis. DRBM is influential in the pre period and also appears in the top five for the during period but does not appear at all in the post period.

Also noticeable, the degree, eigenvector and closeness values for every stock increase during the crisis period, whereas betweenness values decrease. Higher degree and eigenvector values indicate that the stocks have more connections and are connected to more influential stocks directly or indirectly during the pandemic. The higher closeness values on the other hand mean that transmission efficiency has increased, allowing any impacts on one stock to influence other stocks at a faster rate. According to Khoojine and Han (Khoojine & Han 2019), the vertices of a network get closer to one another during a crisis. Therefore, risk is inevitably spread around the network rapidly, leading to an increased chance of systemic risk. Besides that, lower betweenness indicates the absence of structural holes in the network, leading us to believe that the stocks have higher clustering coefficients and are more tightly correlated to one another. It is said that periods of high turbulence lead to high sensitivity and connectivity of vertices (Lai et al. 2021). Overall, the pandemic has caused a change in centrality value magnitude, indicating increased sensitivity, closer proximity between stocks, accelerated transmission rates and increased grouping capabilities.

For degree centrality, DRBM dominates the pre period with 63 connections, followed far behind by LAYH with 56 connections. DRBM then drops to fourth place in the during period, albeit its

higher value of 67, and unfortunately is no longer ranked in the top 5 afterwards. Central stocks in the during period are BESH and MATE, both sharing the highest degree value of 70. This value is 7 and 6 connections higher than the top ranked stock in the pre and post periods respectively. GENM is the most influential stock in the post period with 64 connections, followed closely by GENT with 61 connections. GENT also appears in the third spot in the pre period, whereas ONLY makes two appearances for degree centrality. GENT and ONLY are adversely affected by the crisis, only to arise once again once the crisis has passed. No other stocks appear more than once, signifying a restructuring of the network due to the pandemic. Since, GENM, MFMS and FPIB enter the top 5 list after the crisis period, it's safe to say that the number of their adjacent stocks have increased after the crisis.

Moving on to eigenvector centrality, LAYH is in a central position in the pre-COVID-19 period, with a value of 1.000. However, it is nowhere to be seen in the two periods that follow. The uppermost ranked stocks for each period differ, with OTLS and GENM topping the table in the during and post periods respectively. Interestingly, the only stocks that appear twice for eigenvector centrality, are the same stocks that appear twice for degree centrality in the same periods, namely DRBM, ONLY and GENT. Moreover, only one stock differs for each period between the degree and eigenvector centralities' top 5. This finding makes sense since eigenvector centrality is a natural extension of degree centrality after all. The top ranked stocks are said to have many important stocks connected to them.

Subsequently, not much can be said about the closeness centrality as their values are constant for the top 5 in each period. Only the fifth ranking stock in the post-COVID-19 period has a smaller value than the top 4 stocks. Thus, in this post period, GENM, GENT, MFMS, and ONLY are the most influential stocks in terms of closeness. These stocks have the closest proximity to the other stocks in the network. Similar closeness among the top 5 stocks could mean that the stocks all have the same distance from themselves to the other stocks in the network. Crisis is spread at an equal rate through each of the stocks listed.

For the final centrality, the betweenness values reveals that once again, only DRBM, GENT and ONLY appear twice across all three periods. DRBM tops the table with a value of 0.044 in the pre period but drops two spots in the during period with a value of 0.027. In the during period, it is replaced by GNCH with a betweenness value of 0.036, which is the lowest first place value among

all periods. GNCH is not spotted in the following period. Then there is GENT with a value of 0.050 in first place in the post period, showing the highest betweenness value recorded among all stocks in every period. This shows GENT's utmost importance as an intermediary, controlling the flow of information after the crisis.

DRBM, GENT and ONLY constantly appear more than once for all the centralities over all periods. These three stocks are said to dominate the whole Consumer Products and Services sector of Bursa Malaysia in general. Additional observations can be made about the most influential stocks for each period based on all the centrality measures in general. Firstly, it is noticeable that DRBM, GENT and ONLY appear as key players in the pre period, whereas BESH, MATE and DRBM dominate the during period. GENM, GENT, MFMS and ONLY appear in the top 5 for all centralities in the post period, making them influential stocks after the stock market starts to recover. In conclusion, the stocks may not be consistently ranked across periods for each centrality, but there is some consistency in the main stocks for each period across all centrality measures.

Shortest Paths

Geodesic paths, also known as the shortest path between two vertices in a network, is the path with the minimum number of edges. For weighted graphs, shortest paths are paths with the minimum sum of edge weights. Financial networks with shorter paths can transfer information from one stock to another at a higher speed as they are closer to one another. For the purposes of this report, two algorithms, namely Dijkstra's algorithm and Floyd-Warshall's algorithm, are used to find the shortest paths in all the three networks.

For Dijkstra's algorithm, the network is assumed to be unweighted since the algorithm cannot carry out its computation with negative edge weights. Infinite edge weights are also excluded. Thus, only the shortest paths of the giant component are taken into consideration. This algorithm is a single-source shortest path problem, meaning that it can only find the shortest paths from a source vertex $i \in V(G)$ to all other vertices in the network. Thus, the shortest paths are computed only for the most influential stocks of each period, based on centrality measures. The average path length of the whole network, that is the mean of all the shortest paths of every vertex to all other vertices using breadth-first search is also listed in Table 5. The term average path length and

average distance is used interchangeably throughout this report. Similarly, the network is assumed to be unweighted. The average path length acts as an important indicator of the networks' information transmission efficiency.

Floyd-Warshall's algorithm on the other hand, accepts negative edge weights but not negative cycles. Negative cycles occur when the sum of edges is a negative value. Using this algorithm, all pairs of shortest paths can be computed, giving us the shortest path of the network as a whole.

Average Path Length for Real Network

Table 5. [Average path length of the network in each period using Breadth-First Search]

Average Path Length Using Breadth-First Search	
Pre	2.167
During	2.132
Post	2.261

The average path length values are in accordance with the results from Table 3 in that the during crisis period has the smallest value, 2.132. In the during period, it takes on average 2.132 steps for a stock to reach another stock. This is evidence of stocks being more closely connected and thus enhancing information transmission efficiency. The Consumer Products and Services sector of the Malaysian stock market certainly has small average path length values, as the average length of the shortest path between stocks is only a little above 2 for all three periods. This is one of the features of large networks. It coincides with small-world networks in that the average distance between vertices is said to be around six or less steps apart.

Dijkstra's Algorithm

Table 6. [Shortest paths of the most influential vertices in each period based on their centrality measures, using Dijkstra's algorithm]

Pre		During		Post	
DRB-Hicom (DRBM)	1.611	Beshom Holdings (BESH)	1.517	Genting Malaysia (GENM)	1.627
Genting (GENT)	1.704	Magni-Technology Industries (MATE)	1.458	Genting (GENT)	1.640
Only World Group Holdings (ONLY)	1.735	DRB-Hicom (DRBM)	1.492	Malayan Flour Mills (MFMS)	1.696
				Only World Group Holdings (ONLY)	1.727

In the pre-COVID-19 period, DRBM has the smallest shortest path value of 1.611, indicating its closeness to all other stocks in the network. This only emphasises the importance of this stock in the pre period as it also showed impeccable performance based on centrality measures. In addition to that, DRBM's shortest path value is really close to that of MATE in the during period. For the last timeframe, GENM has the smallest shortest path value of 1.627, enhancing its central position in the post-COVID-19 network.

Floyd-Warshall's Algorithm

Table 7. [Shortest path of each network using Floyd-Warshall's algorithm]

Mean Shortest Path Using Floyd-Warshall Algorithm	
Pre	-7.712×10^{109}
During	-166078587
Post	-1.125×10^{116}

The negative mean shortest path values obtained in Table 7 indicate the presence of negative cycles. This renders the Floyd-Warshall algorithm unfit to compute the shortest paths for the networks in this report since it will output incorrect results.

Local and Global Clustering Coefficient for Real Networks

Vertices that have identical neighbours tend to be more related to each other. This can be measured by local clustering coefficients (local CC), showing the probability of neighbours of a vertex to be neighbours themselves. The local CC of a single vertex $i \in V(G)$ is defined as follows:

$$Local\ CC_i = \frac{2E_i}{d_i(d_i - 1)}$$

where E_i is the number of edges between the neighbours of vertex i. Local CC can identify vertices with structural holes, that are missing links between the neighbours of a vertex. It is harder for information to be passed around when there are more structural holes, but the influence of the vertex as a broker in passing information around increases.

The global clustering coefficient (global CC) can be used to calculate the total number of closed triangles in the whole financial network as follows:

$$Global\ CC = \frac{3\ \times (number\ of\ triangles)}{number\ of\ connected\ triplets}$$

Alternatively, the global CC of a network can also be computed by averaging over the local CC values of every vertex in the network, as shown below:

$$Global\ CC = \frac{1}{N}\sum_{i=1}^{n} Local\ CC_i$$

where N is the number of vertices in the network. For the purposes of this report, the first Global CC formula is utilised during analysis.

Local Clustering Coefficient (Local CC)

Table 8. [Top 5 stocks with the highest local clustering coefficient values]

No.	Pre		During		Post	
1	Rhong Khen International (RHOG)	0.600	AHB Holdings (ARTW)	1.000	Tomei Consolidated Berhad (TMEI)	0.667
2	Perak Transit (PERT)	0.497	G3 Global (GLOA)	1.000	Niche Capital Emas Holdings (NICH)	0.500
3	Sinaran Advance Group (SINA)	0.462	Khee San (KHEE)	1.000	Pertama Digital (PERM)	0.500
4	Advance Synergy (ADVA)	0.458	Konsortium Transnasional (KSTM)	1.000	RGB International (RGBI)	0.485
5	Berjaya Land (BLAD)	0.455	Mesb (MESB)	1.000	AirAsia X (AIRX)	0.473

It is easier for grouping and clustering to happen between vertices with higher local CC values. Stocks with high clustering coefficients hold a dominant position in the financial networks as they can easily infect other stocks with any good or bad effects at a faster rate of contagion. Special attention must be paid to ARTW, GLOA, KHEE, KSTM and MESB as they show the maximum local CC value possible, portraying their ability to quickly affect the other stocks in their cluster during troubled periods. With a local CC value of 1, the neighbours of these stocks are certain to form triangles among themselves, thus leading to the absence of any structural holes.

In the pre and post periods, RHOG and TMEI certainly do show much higher local CC values than the other stocks, at 0.600 and 0.667 respectively. The other stocks in these two periods show nearly similar values, which are also quite high. None of the stocks consistently attain high local CC values in all periods, since none of them appear twice in Table 8. The emergence of a crisis certainly does affect the clustering capabilities of the stocks in the Consumer Products and Services sector.

Global Clustering Coefficient (Global CC)

Table 9. [Global clustering coefficient values for each of the three real networks]

	Global CC
Pre	0.307
During	0.621
Post	0.315

Table 9 shows that the global CC values during the crisis period soars to double its values in the pre and post-COVID-19 periods. The pre and post periods can be said to have similar global CC values. This indicates that the stocks find it easier to form cliques during times of crisis. Similar findings can be found in a study by Luo (2022), where the global CC of banking networks during the COVID-19 period were significantly higher than any other period. Besides that, Kumar et al. (2022) also found that during the sub-prime crisis of 2008, the global CC values of DJIA stocks were clearly higher than the pre and post crisis periods.

Comparing Table 3 and Table 9, it can be seen that the global CC of each network is much bigger than the density of the networks:

i. Global CC of pre period = 0.307 >> 0.112 = Density of pre period
ii. Global CC of during period = 0.621 >> 0.118 = Density of during period
iii. Global CC of post period = 0.315 >> 0.103 = Density of post period

Therefore, all three COVID-19 networks have a high clustering coefficient, which is one of the characteristics of a small-world network. This finding also coincides with the fact that the average path length during the crisis period is the lowest according to Table 5. All in all, there are significant changes in the structure of the network brought forth by the crisis, in that periods of turmoil constantly strengthen the correlation between stocks. Higher clustering coefficients could be due to higher dependence of stocks on each other during a crisis. This leads to groups of stocks with similar characteristics, for example, how their prices fluctuate. Thus, it could be quite difficult for investors to diversify their networks during crisis periods as the stocks tend to herd and behave similarly.

Degree Distribution of Real Networks

For undirected networks like the real networks in this report, the degree distribution is the sequence $P(k_i = 0), P(k_i = 1), P(k_i = 2), ...$, where $P(k_i = k)$ is the probability of vertices in the graph having a degree of *k*. By calculating how many vertices have a degree of 0 or 1 or 2 and so on before dividing them by the total number of vertices, we get the degree distribution. All these probabilities must then sum up to one. Degree distributions are very helpful to help us capture a certain aspect of the structure of networks, whether they have a binomial distribution (small networks), Poisson distribution (large networks) or even a power law distribution. However, they are not able to tell us how all these vertices are connected to one another. Here on forth, the terms real networks and stock networks are used interchangeably.

Bar Plot on A Linear Scale

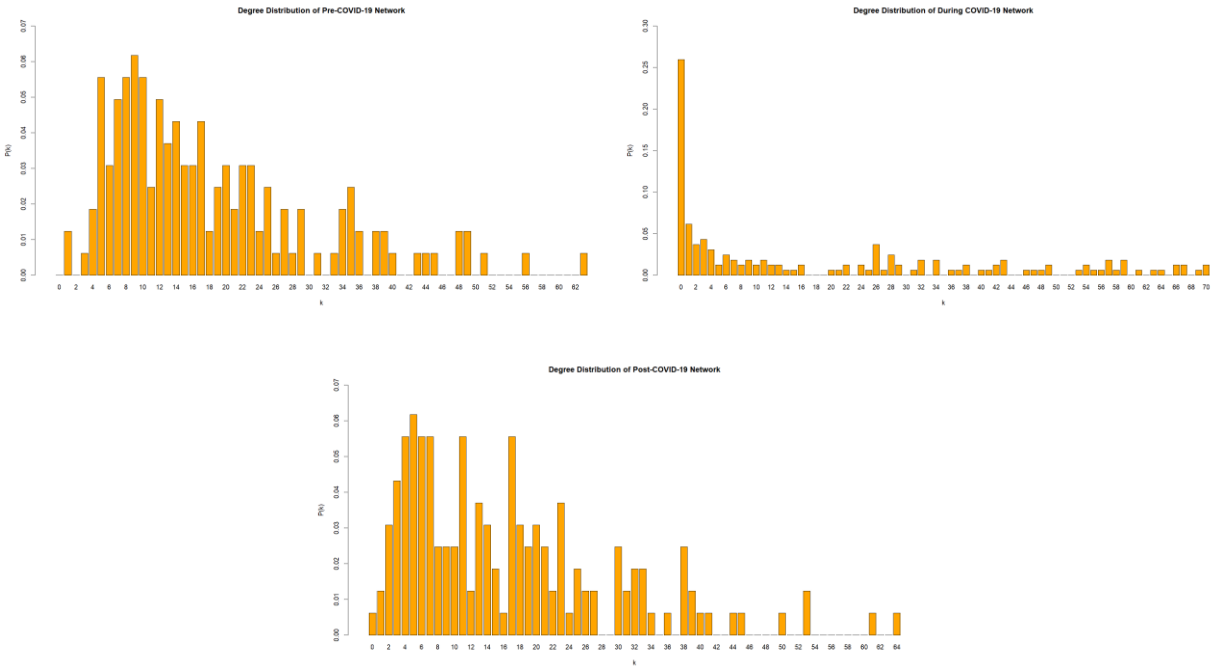

Figure 7. [Degree distribution bar plot of real networks in the pre, during and post-COVID-19 periods on a linear scale]

The first thing observed is that the pre period has no isolated vertices, whereas that of the during period is the highest. This has already been explained earlier in the threshold network plots subsection. All three networks can be said to follow a power law distribution, a distribution that is obeyed by many different kinds of real networks. However, the during COVID-19 period certainly portrays a much more extreme structure compared to the pre and post periods which have somewhat similar structures. In the during period, after a degree value of 4, the vertices seem to be evenly distributed across different number of connections. The pre-COVID-19 period bar plot shows us that the greatest number of connections a vertex can have is k = 63 with $P(63) = 0.0062$. For the during and post period, they are $P(70) = 0.0123$ and $P(64) = 0.0062$ respectively.

Scatterplot on a Log-Log Scale

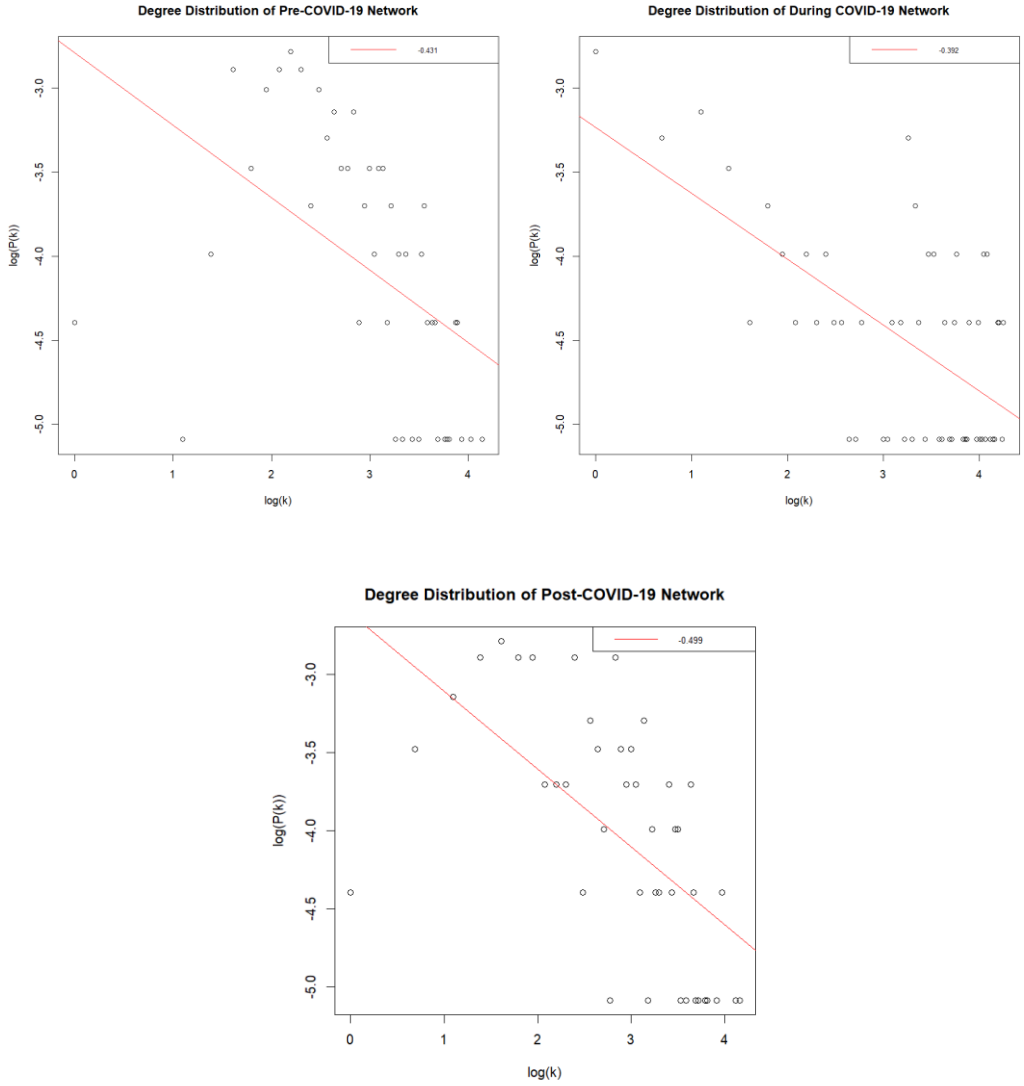

Figure 8. [Degree distribution scatterplot of real networks in the pre, during and post-COVID-19 periods on a log-log scale]

By plotting the degree distribution of a real network on double logarithmic axis (log-log plot), the power law will follow a straight line. It is evident that the network certainly does not follow a binomial distribution as no bell curve shape can be seen. The vertices seem to form a line, although they are quite scattered around the fitted line (red line). The vertices are especially scattered for the during period, as can be seen in the bar plot above too.

The power law distribution can be represented by $P(k) = Ck^{-a}$, where a is the degree exponent that can be represented simply by the value of the slope in the plot. A higher a value or a steeper slope would mean that the number of vertices with high degree is smaller than the number of vertices with low degree. The network in the post-COVID-19 period has the steepest slope (highest degree exponent), whereas the network in the during period has the lowest degree exponent value. Anyway, the degree exponent values in each network are not that far apart, indicating a power law distribution of the networks with a scale free behaviour. To conclude this subsection, the networks slightly follow the power law distribution, thus they can be said to be scale-free.

C(k) Distribution for Real Networks

In order to capture the hierarchical nature of the three financial networks produced, their C(k) distributions are plotted. These plots show the average clustering coefficient of nodes with a degree of k, C(k), that is the value of the average local CC as the degree value (number of connections a stock has) increases. In most networks, local CC is found to have a rough dependence on degree, where the C(k) distribution follows a power law. This means that vertices with more connections have lower local CC on average. However, we see in the three real networks below that this is not always the case.

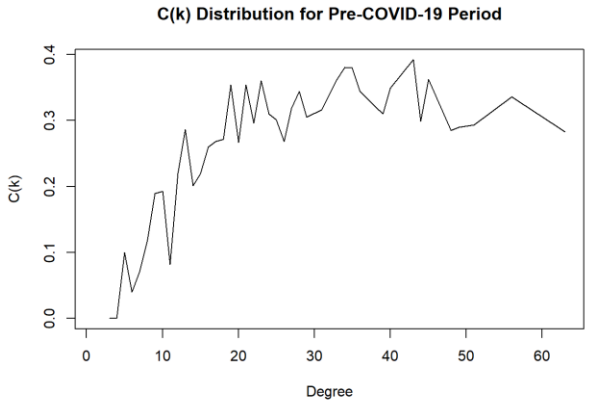

Figure 9. [C(k) distribution plot of the pre-COVID-19 network]

From Figure 9 above, the C(k) values range from 0 to 0.4. The pre-COVID-19 period has a C(k) distribution with an increasing hierarchy up to around a degree value of 20, before showing a somewhat constant trend. This indicates that as the stocks have an increasing number of

connections up to around 20, their ability to form clusters increases as well. However, the average local CC of stocks with more than 20 connections portray a weak dependence on their degree values. They show an average local CC of around 0.3, meaning that there is a 30% chance for the neighbours of vertices with more than 20 connections to be connected among themselves.

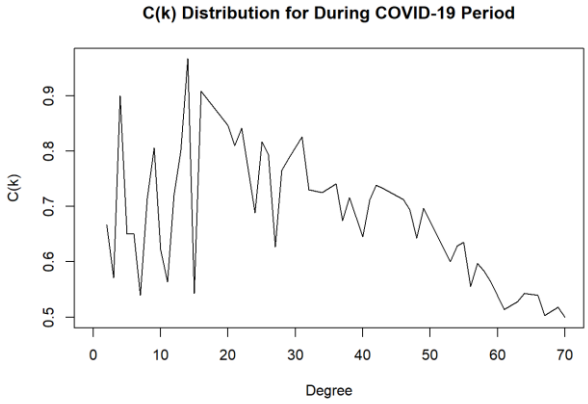

Figure 10. [C(k) distribution plot of the during COVID-19 network]

The lowest C(k) value of this network is 0.5, whereas the highest reaches a value of nearly 1, showing certain clustering among neighbours of vertices. The C(k) distribution of the during COVID-19 period displays an erratic trend, increasing and decreasing with a great variance up to a degree value of 30. Due to this erratic trend, it looks somewhat constant around 0.75, before showing a decreasing hierarchy. As the number of connections a stock has increases after the value 30, the ability of the stocks to form clusters decrease to 0.5 at a degree value of 70. This network exhibits the properties of common networks after the degree value of 30.

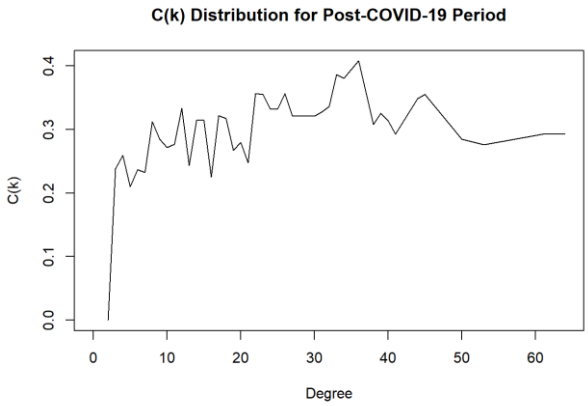

Figure 11. [C(k) distribution plot of the post-COVID-19 network]

Although there are slight increases and decreases of C(k) values in the plot from Figure 11, the network can be labelled as a constant network showing no hierarchy for the most part. Similar to the pre-COVID-19 network, the average local CC value is constant around 0.3. No matter how many other stocks a stock is connected to, their ability to form triangles is 30%. Here, small or large degree values do not affect the clustering ability of vertices.

All three networks show different C(k) distribution patterns, indicating how the pandemic has caused much turmoil even in clustering abilities of stocks. A very obvious observation can be made in the fact that the C(k) values of the during COVID-19 network are tremendously higher compared to the two other networks. Even its lowest C(k) value, 0.5, is higher than the maximum C(k) values of the pre and post-COVID-19 periods. This indicates that during a crisis, stocks tend to cluster and have strong relationships with each other. Therefore, positive or negative spillovers can easily spread from one stock to another as they huddle up together. The pre and post-COVID-19 networks have a similar C(k) constant of 0.3, which might be the usual clustering ability of stocks during calm periods of time. The during and pre-COVID-19 networks show totally opposite C(k) distribution patterns, indicating that the stock market took a large hit during the crisis and causing unpredictable outcomes.

Random Network: G(N,p)

The structure obtained from the three stock networks can be compared to the predictions of a random network, G(N,p), also known as the Erdős Renyi random graph. G(N,p), is a simple and unweighted graph of *N* vertices, where each pair of vertices is connected by an edge with a preset probability of *p*. these edges are assumed to be independently and identically distributed. The degree distribution of a random network should follow a binomial or Poisson distribution since they do not have any hubs.

The clustering coefficient of a random network on the other hand can be mathematically defined as

$$C = \frac{number\ of\ closed\ triplets}{number\ of\ triplets} = p = \frac{<k>}{N-1}$$

since in a random graph, the probability that any two vertices are adjacent is exactly the same. The probability that an edge forms between any two vertices is exactly *p*. The clustering coefficient of random networks are said to underestimate with orders of magnitudes the clustering coefficient of real networks since large random networks do not tend to cluster. The bigger a random network, the smaller its global clustering coefficient, to a point it practically vanishes.

Real networks and random graphs are similar in terms of having short distances as the size of the network increases. The average distance among vertices in a random graph based on the small-world effect is logarithmically small and can be calculated as follows:

$$< d > \; = \; l_{rand} \approx \; \frac{\ln N}{\ln < k >} \; .$$

For all the random graphs generated, *p* is set as the clustering coefficient of the real network. The three random networks in this study are G(162, 0.112), G(162, 0.118) and G(162, 0.103).

Figure 12. [Random networks of the pre, during and post-COVID-19 periods]

The three random networks generated for the pre, during and post periods with a preset probability, *p* of 0.112, 0.118 and 0.103 respectively, are shown in Figure 12. Since the during period has the highest probability for edges to form between vertices, it is only logical for the random network of the during period to have the greatest number of edges at 1578. This is due to the fact that there is a higher chance for edges to form between the pairs of all 162 vertices in the network. The same can be said for the network in the post period that has the smallest number of edges due to its lower preset probability. The number of edges formed in the random networks are in line with the number of edges in the real networks.

Degree Distribution for G(N,p) Networks

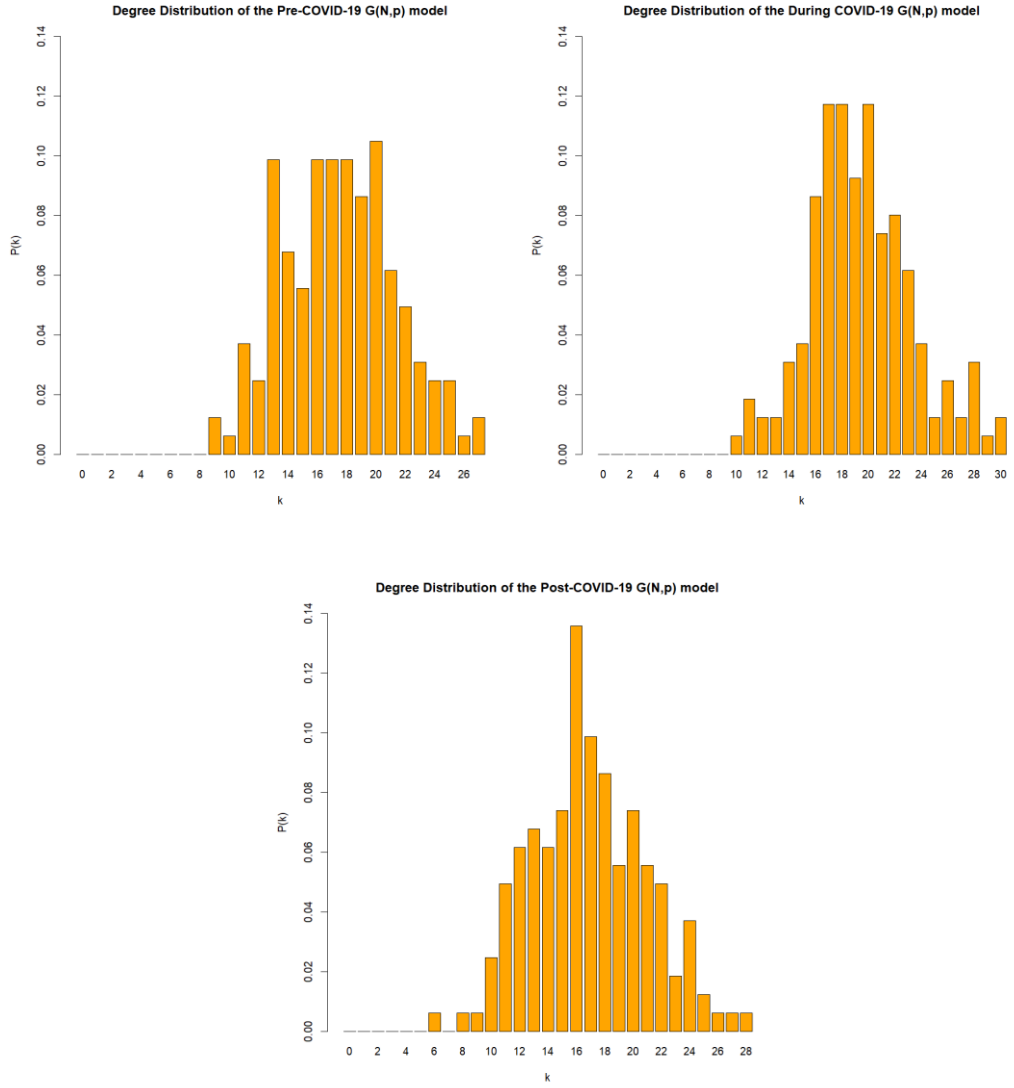

Figure 13. [Degree distribution bar plot of random networks in the pre, during and post-COVID-19 periods on a linear scale]

All three random networks portray a very clear obeyance of the binomial distribution. The highest degree distribution probability is seen to cluster about the mean. This indicates the absence of hubs in the random networks that would otherwise be present in real networks. Hubs are absent due to the fact that random networks assume a fixed number of vertices, whereas in real networks, the number of vertices are continuously growing. Besides that, random networks have a fixed probability, *p*, for edges to form between vertices. This however does not happen in real networks where vertices tend to attach to other vertices with a higher degree. It could be that in stock

networks, the stocks tend to connect to other stocks that could boost their stock prices, forming hubs.

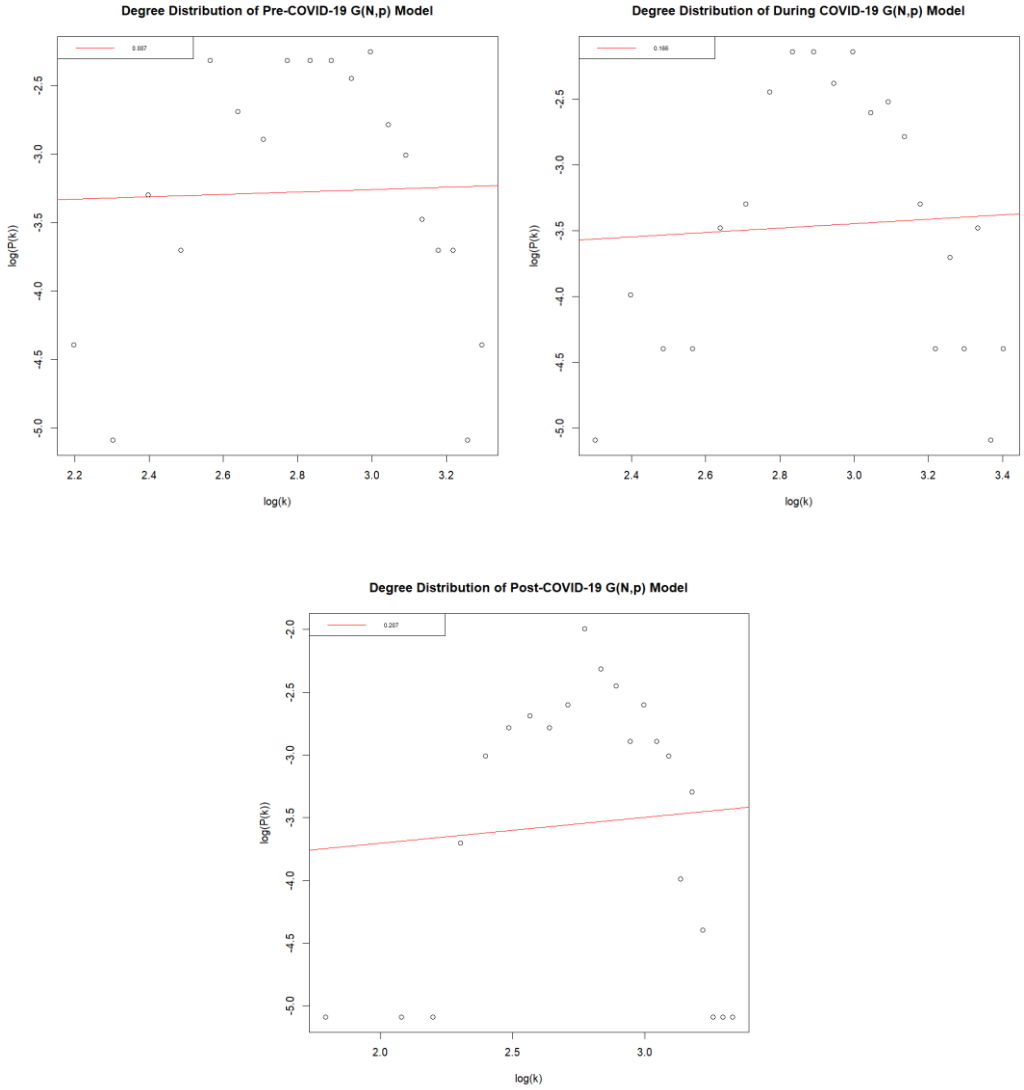

Figure 14. [Degree distribution scatterplot of random networks in the pre, during and post-COVID-19 periods on a log-log scale]

On a log-log scale, the scatterplot certainly shows that all three random networks are curved in a bell shape manner. Since the size of the network is not that large, the random networks are said to follow a binomial distribution instead of a Poisson distribution. In random networks, most of the vertices would have around the same degree values, whereas a few vertices would have either small or large degree values.

Global CC for G(N,p) Networks

Table 10. [Global clustering coefficient values for each of the three random networks]

Global CC for	
Pre	0.108
During	0.116
Post	0.106

Table 10 proves that the global CC for random networks do in fact underestimate the magnitude of the global CC values of real networks. This is a pattern found in real networks that deviate from the predictions of a random network model. The stock networks in the during period had the highest global CC value that was double the pre and post periods. Even though this is not reflected in the global CC for the random networks, their values are still slightly higher in the during period.

Average Path Length for G(N,p) Networks

Table 11. [Average path length of the three random networks using Breadth-First Search]

Average Path Length Using Breadth-First Search	
Pre	2.021
During	1.959
Post	2.055

The average path lengths of all three random networks are in the vicinity of the value 2, with the during period having the smallest value, similar to the real networks. With a small average path length, information transfer between vertices can be done much more efficiently and quick. All the pre, during and post random networks have a small clustering coefficient and average path length.

Watts-Strogatz Network : WS(N,k,p)

The Watts-Strogatz network (WS network) discovered by Duncan Watts and Steven Strogatz in 1998, also famously known as the small-world network, is an extension of the random graph.

Before its discovery, it was assumed that the topology of networks was either completely regular or completely random. However, many real networks seemed to be in the middle of these two extremes with high global CC values like regular networks and small average path lengths like random networks (Watts & Strogatz 1998). The WS network basically involves rewiring of the regular network with probability *p*. This introduces disorder in the network to make it lie somewhat between the regular network and a random network.

The values of *k* to generate the WS networks are set to the average degree of the respective real networks, while the values of *p* are similar to the ones utilised in generating random networks. By increasing the value of *p*, randomness increases to a point the regular network turns into a random network when $p = 1$. This is demonstrated in Figure 16. The three WS networks in this study are WS(162, 18.074, 0.112), WS(162, 19.062, 0.118) and WS(162, 16.630, 0.103).

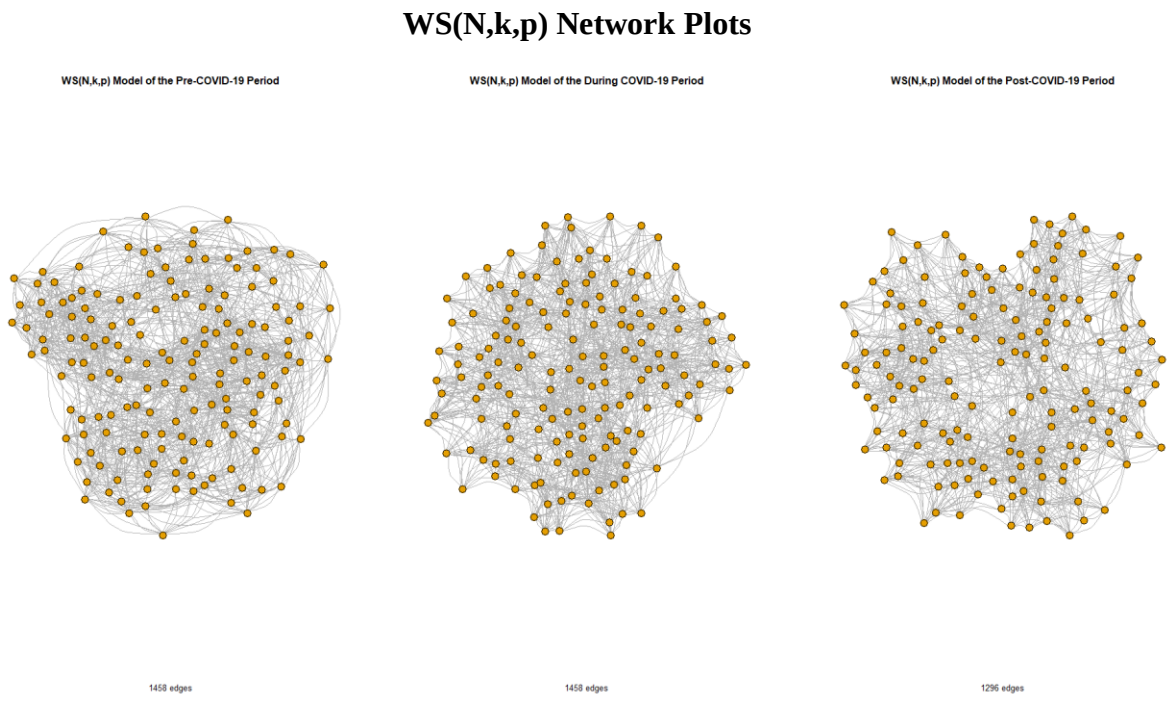

Figure 15. [WS(N,k,p) networks of the pre, during and post-COVID-19 periods]

As the pre and during COVID-19 periods have roughly similar average degrees of 18.074 and 19.062 respectively, the pre and during WS networks that have been generated have the same number of edges. The WS network in the post period however, has less edges due to its smaller

average degree value of 16.630. The following subsections will show how the stock networks in this report are similar to these three WS networks generated.

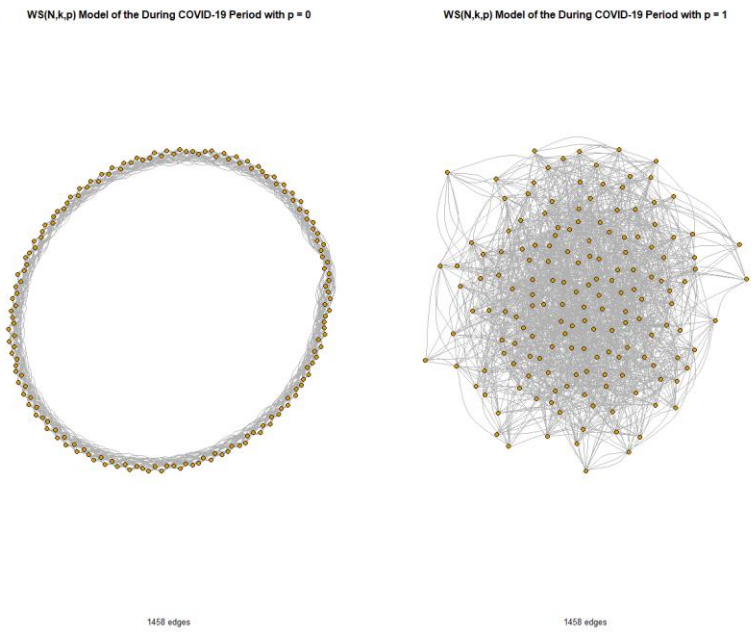

Figure 16. [WS(N,k,p) networks of the during COVID-19 period with $p = 0$ and $p = 1$]

To enhance our understanding of small-world networks, Figure 16 portrays WS networks of the during period that have been generated using a p value of 0 and 1 respectively. With a rewiring probability of 0, the edges do not rewire at all, meaning that the network generated is merely a regular graph with high clustering and low average path lengths. All of the vertices have the same degree values that are equal to the average degree. On the other hand, with a rewiring probability of 1, the network is a random one. This is because every single edge will definitely be rewired to a new position. By introducing the perfect range of p values, small-world networks can be formed, lying in between these regular and random networks.

Degree Distribution

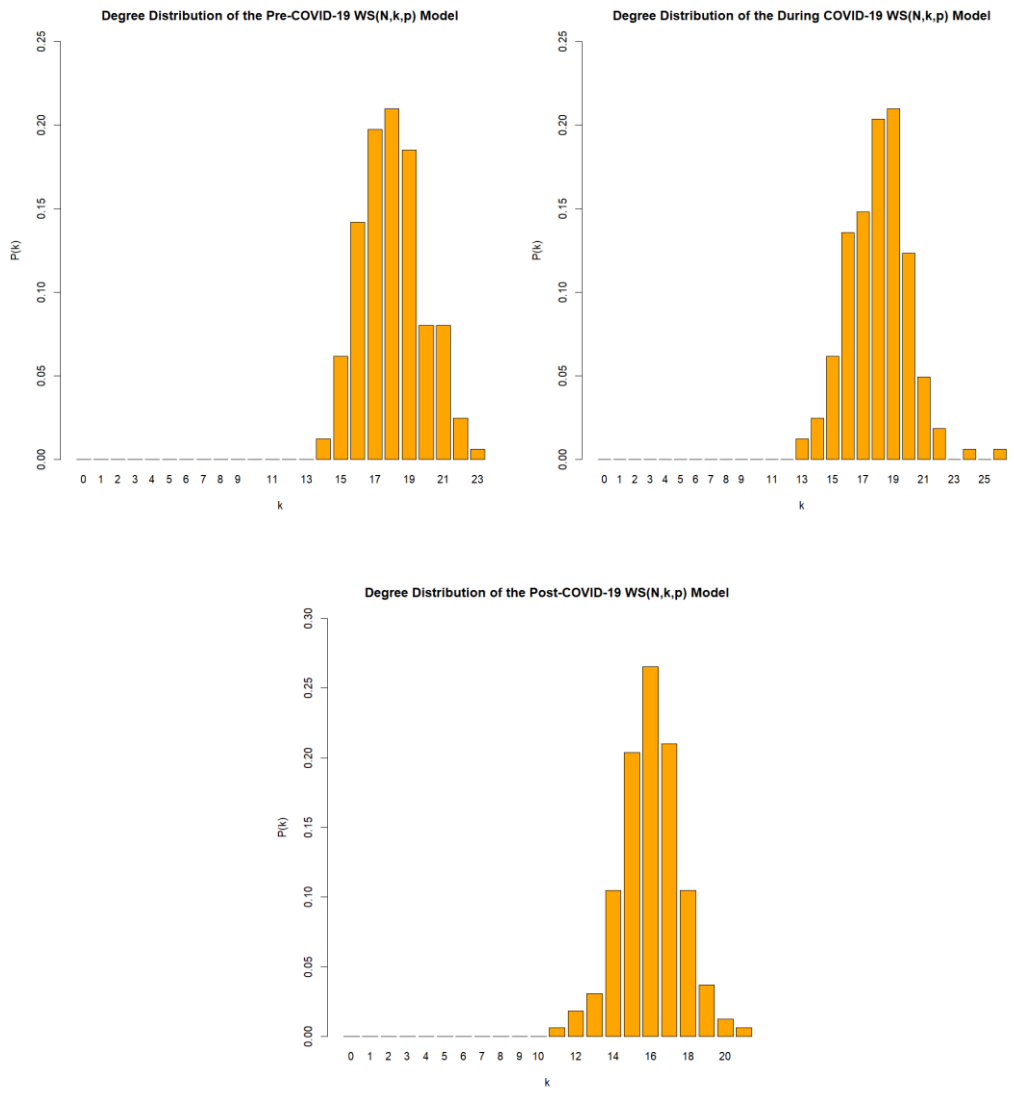

Figure 17. [Degree distribution bar plot of WS(N,k,p) networks in the pre, during and post-COVID-19 periods on a linear scale]

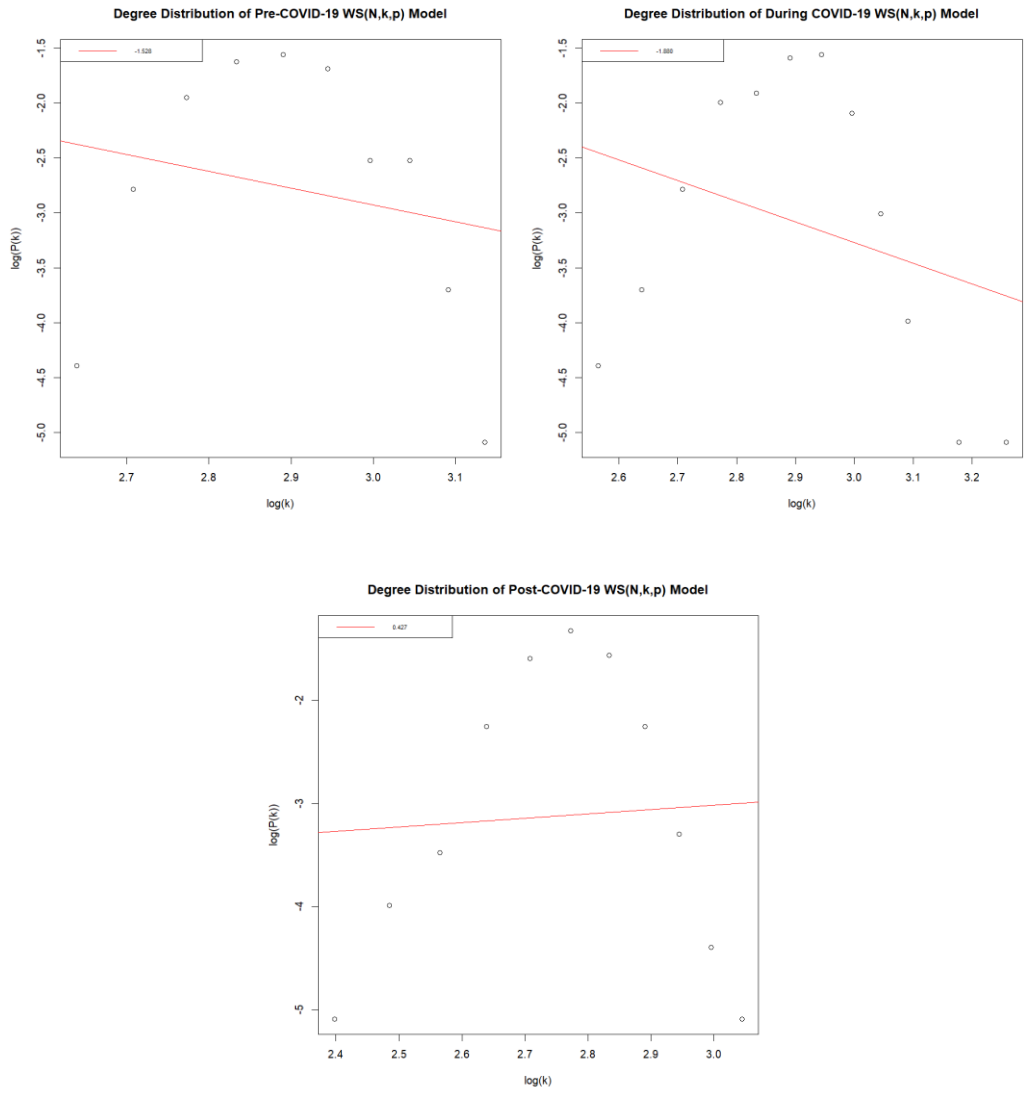

Figure 18. [Degree distribution scatterplot of WS(N,k,p) networks in the pre, during and post-COVID-19 periods on a log-log scale]

Being an extension of the random network, the WS networks also predict a binomial bounded degree distribution as can be seen in Figure 17 and Figure 18. Most of the vertices have a degree value of 18, 19 and 16 in each network respectively. There are not too many vertices with high or low degree values. From the scatterplots, it is noticeable how poor of a fit the power law distribution is to the degree distribution of networks in all three periods.

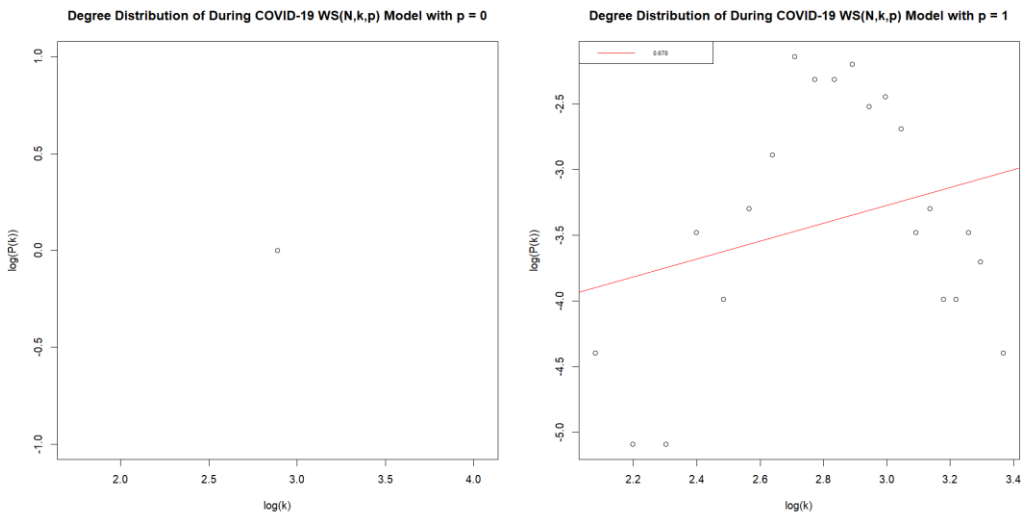

Figure 19. [Degree distribution scatterplot of WS(N,k,p) networks during COVID-19 period with $p = 0$ and $p = 1$]

Degree distribution scatterplots of WS networks on a log-log scale in the during COVID-19 period with p values of 0 and 1 can be seen in Figure 19. In the first scatterplot, there is only one point plotted. This is in line with the fact that when there is no probability for the edges to rewire, the network remains as a regular graph with every vertex having a degree equal to the average degree. On the contrary, with a certain rewiring probability of 1, the network becomes a random network that follows a binomial distribution.

Global Clustering Coefficient (Global CC)

Table 12. [Global clustering coefficient values for each of the three WS(N,k,p) networks]

	Global CC
Pre	0.373
During	0.361
Post	0.377

The global CC values of all three WS networks are much higher than that of the random networks. The values are in par with those of the real networks, except for the during period for which its

value does not double. Nevertheless, the real networks seem to show similarities with the WS networks in terms of having high clustering properties.

Average Path Length

Table 13. [Average path length of the WS(N,k,p) network in each period using Breadth-First Search]

Average Path Length Using Breadth-First Search	
Pre	2.216
During	2.211
Post	2.327

The WS networks have small average path lengths of around 2 for each period, similar to the stock networks and random networks in this report. The post period network has an average path length of 2.327, being the largest value while the smallest average path length is in the during period. These average path length values show similar patterns to those in the stock network, stipulating that the WS networks are a good reference for the stock networks generated.

Barabasi-Albert Network : BA(N,k)

The Barabasi-Albert network (BA network) can explain the lack or absence of hubs and power laws in random networks. In random networks, there are two hidden assumptions that are violated by real networks. These random networks assume that networks all have a fixed number of vertices besides assuming that edges are randomly formed with a probability, p. However, real networks differ from random networks in those two very essential aspects. In real networks, there is actually growth where the size of the networks continuously grows with the addition of vertices over time. The vertices being added to the network also do not randomly form edges, instead they tend to form connections with other vertices that have a high degree. This is called preferential attachment, a term coined by Barabasi and Albert to explain the origin of scale-free networks. Here, the

probability $\Pi(k)$ that an edge of a new vertex connects to vertex i depends on the degree, k_i, as shown below:

$$\Pi(k_i) = \frac{k_i}{\sum_j k_j}.$$

Thus, growth and preferential attachment play an essential role in shaping the degree distribution of networks. The three BA networks generated for each period are BA(162, 18.074), BA(162, 19.062) and BA(162, 16.630).

BA networks have a power law degree distribution in nature, whereas their average distance is smaller than the average distance observed in a random graph of similar size. This is because the average distance grows slower than *ln N* as shown below:

$$\langle d \rangle \approx \frac{\ln N}{\ln \ln N}.$$

Next, BA networks are locally more clustered than a random network as their clustering coefficient increases for large *N* as follows:

$$C \sim \frac{(\ln N)^2}{N}.$$

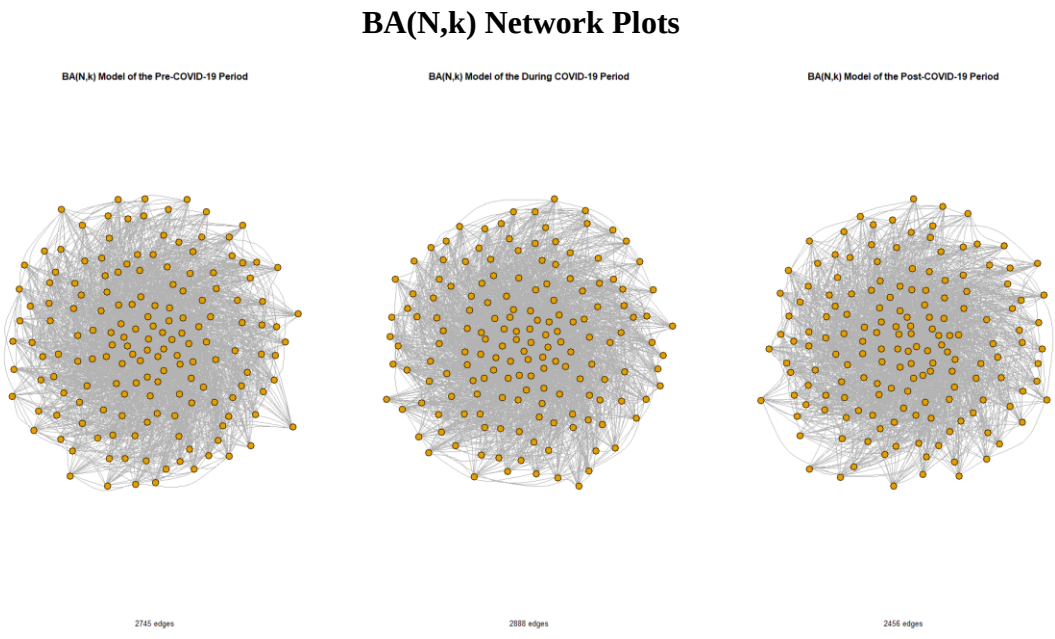

Figure 20. [BA(N,k) networks of the pre, during and post-COVID-19 periods]

The three BA networks generated as shown in Figure 20 display a similar pattern to the stock networks in terms of the number of edges formed. The during period network has the greatest number of edges at a value of 2888, whereas the post period network has the least number of edges at 2456.

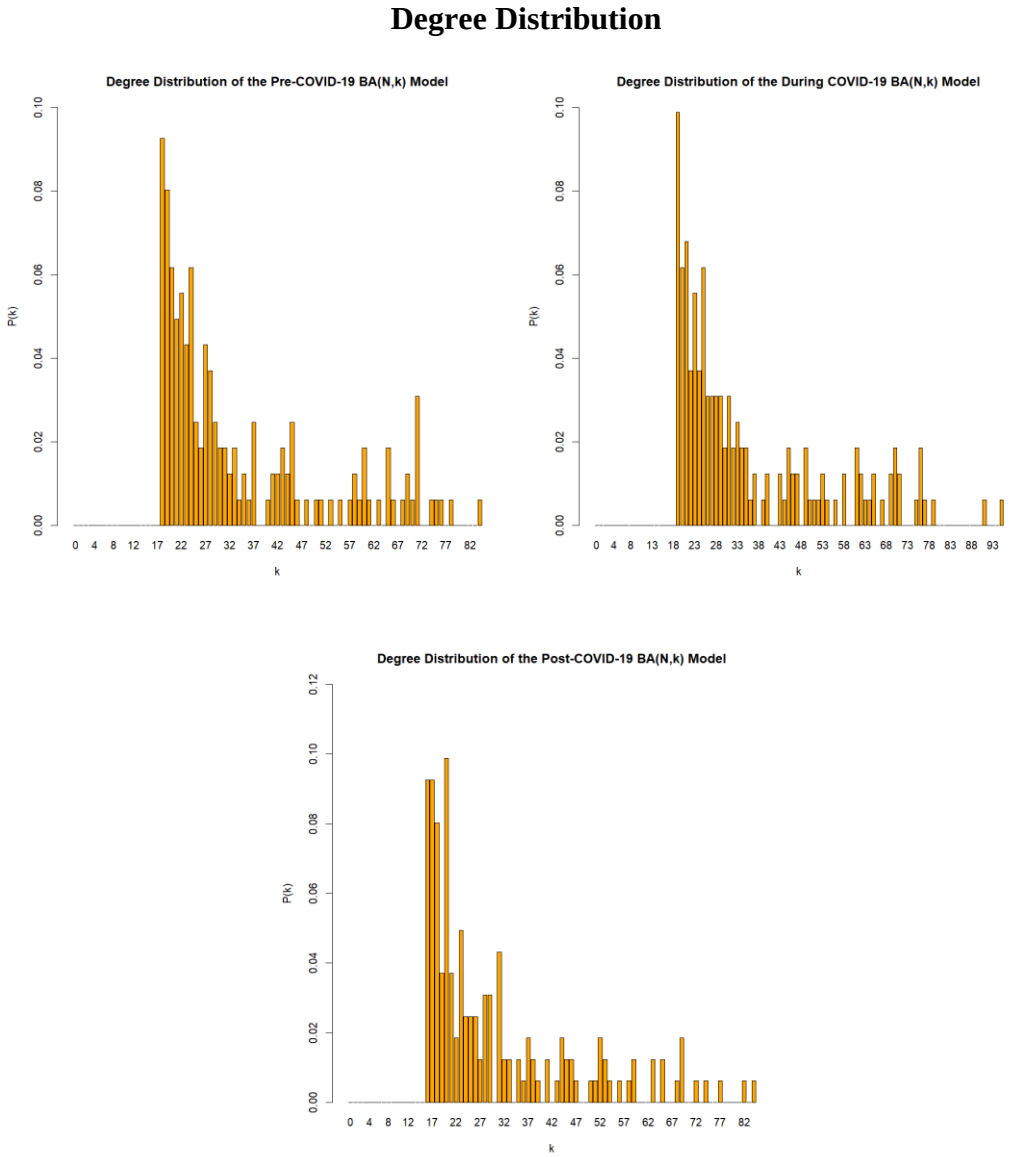

Figure 21. [Degree distribution bar plot of BA(N,k) networks in the pre, during and post-COVID-19 periods on a linear scale]

Similarly to the stock networks, the BA networks' degree distribution is well approximated using power law. Power law is however an even better fit for the BA networks. This indicates the

presence of many vertices with lower degree values and also hubs that could dominate the network as seen in the fat tails of the bar plot.

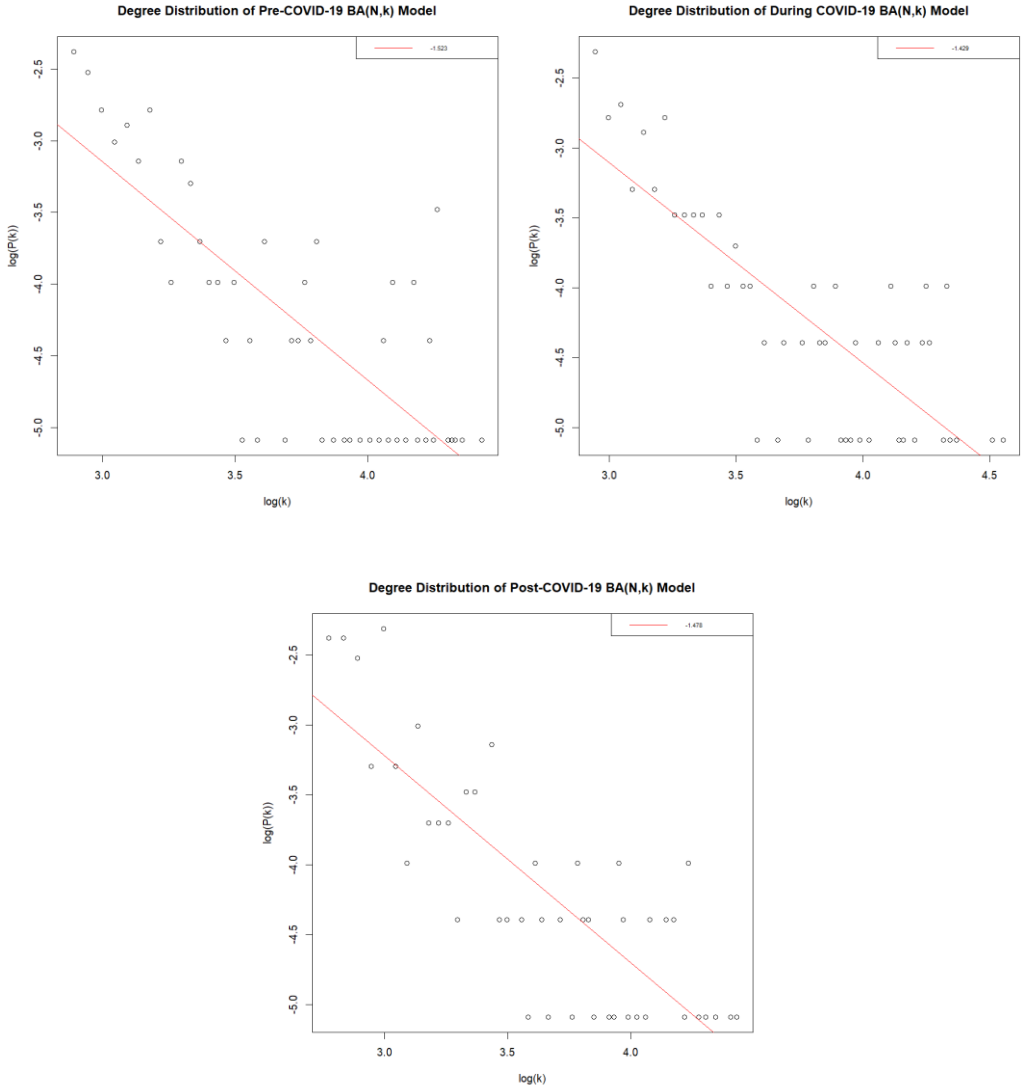

Figure 22. [Degree distribution scatterplot of BA(N,k) networks in the pre, during and post-COVID-19 periods on a log-log scale]

Notice how the points in the scatterplot arrange in a line rather than have a bell curved shape. The networks follow a power law distribution with the pre period network having the highest degree exponent value. Nevertheless, all the degree exponent values are very close to each other, portraying their scale free behaviour. The power law nature of BA networks would be even more obvious as the networks get larger.

Global Clustering Coefficient (Global CC)

Table 14. [Global clustering coefficient values for each of the three BA(N,k) networks]

	Global CC
Pre	0.327
During	0.339
Post	0.302

The global CC values of the BA networks range from 0.302 to 0.339, with the highest value being possessed by the network in the during period. These values are about as high as those of the stock networks but the during period global CC still does not capture the extreme increase shown by the stock network in the during period (0.621). These BA networks are locally more clustered than random networks.

Average Path Length

Table 15. [Average path length of the BA(N,k) network in each period using Breadth-First Search]

	Average Path Length Using Breadth-First Search
Pre	1.795
During	1.781
Post	1.822

The average path length values computed by the BA networks are smaller than those computed in the previous stock, random and WS networks, even though all the networks have the same size. The small path length makes it easier for information to flow through the network at a faster rate.

Configuration Model: G(N, $\bar{k}$)

Configuration models can help us to determine how much of observed patterns in a network are driven by the degrees of the network. To construct a configuration model, the degree sequence,

$\bar{k} = \{k_1, k_2, \ldots, k_N\}$, of the real network must be provided to generate a random network, where all the vertices have the same degree values. The sum of the degree values of all the vertices, $\sum_{i=1}^{N} k_i$, must be even. Even though all the vertices have the same degree values as the real network, the vertices are linked together randomly, as long as the degree values are not affected. Configuration models can also be addressed as random networks with pre-defined degree. Values of real networks that deviate from the values provided by the configuration model indicate that these values are not solely influenced by degree.

For the configuration models in this section, an ensemble of 10 configuration models are generated with the degree sequence of the respective stock networks. The betweenness centrality, eigenvector centrality and global CC values of these 10 models are averaged and then compared to those of the stock networks in each period.

Table 16. [Top 5 betweenness and eigenvector centrality values for the stock and configuration model networks in each period]

Betweenness Centrality (Top 5 Values)					
Pre		During		Post	
Real Network	Configuration Model	Real Network	Configuration Model	Real Network	Configuration Model
0.044	0.064	0.036	0.060	0.050	0.072
0.037	0.049	0.032	0.052	0.045	0.063
0.036	0.037	0.027	0.043	0.042	0.050
0.036	0.037	0.023	0.042	0.039	0.044
0.032	0.036	0.023	0.041	0.032	0.044
Eigenvector Centrality (Top 5 Values)					
Pre		During		Post	
Real Network	Configuration Model	Real Network	Configuration Model	Real Network	Configuration Model
1.000	1.000	1.000	0.996	1.000	0.975
0.922	0.893	0.969	0.980	0.991	0.947
0.799	0.853	0.937	0.970	0.755	0.851

0.791	0.823	0.910	0.964	0.671	0.813
0.704	0.807	0.890	0.962	0.617	0.796

In Table 16 above, the top 5 betweenness and eigenvector centrality values for the stock networks and configuration model networks in each period are listed down. Even from these top 5 values, it is roughly seen that the values provided by the configuration models are higher than those of the real networks. In order to access these comparisons over the whole network more conveniently, Figure 23 and Figure 24 show line plots of the betweenness and eigenvector centrality values of both the stock network and configuration model network in the same plot. Besides the difference in magnitude of values, the structure or pattern of the values can also be assessed.

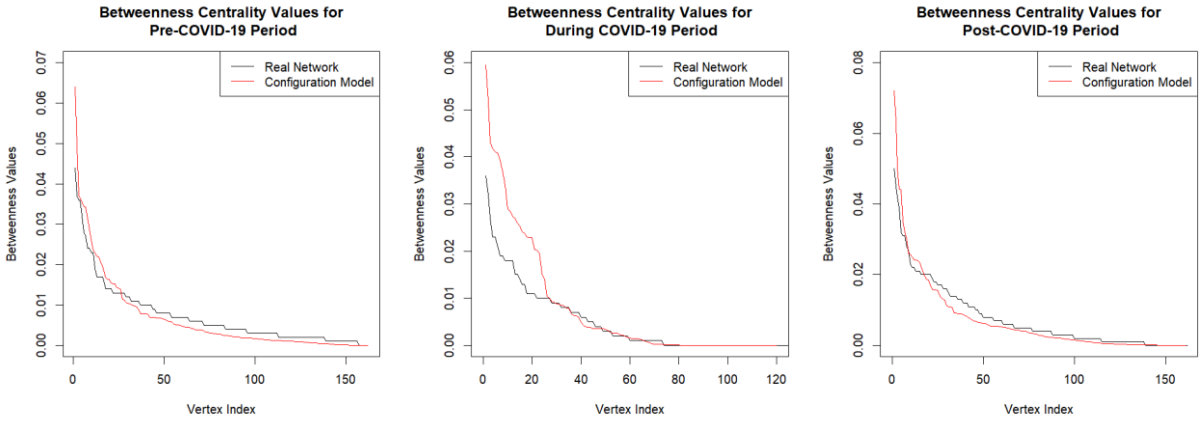

Figure 23. [Comparison of the betweenness centrality values for all the vertices in the real and configuration model networks of each period]

For all three periods, the betweenness centrality values for the configuration model start off higher and later on is below the stock network values. This is more distinct in the during period where the betweenness values start off much higher in the configuration model and then is similar to that of the stock network around vertex index of 25 onwards.

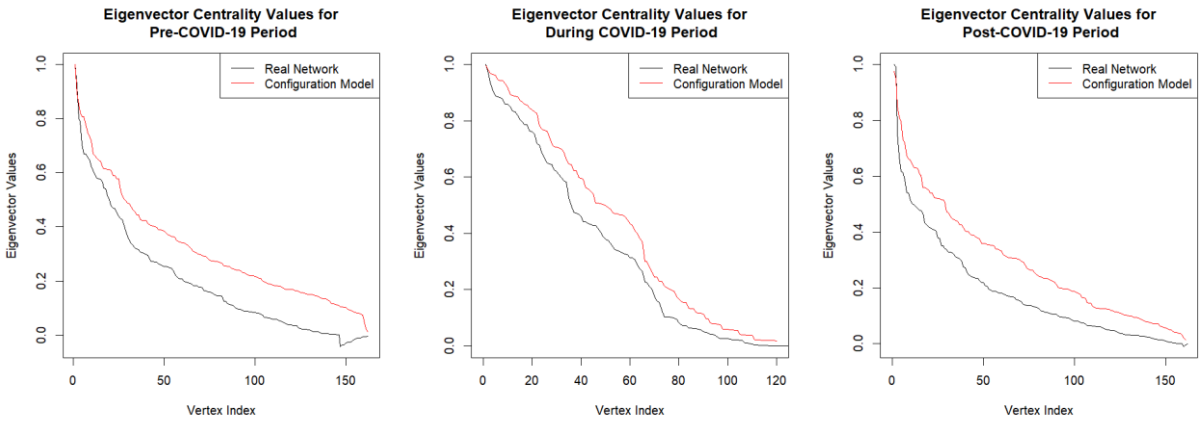

Figure 24. [Comparison of the eigenvector centrality values for all the vertices in the real and configuration model networks of each period]

From Figure 24, it is clearly apparent that the eigenvector centrality values of the configuration model networks are generally higher than that of the stock networks, except for the first few vertices. In spite of these findings, if one were to look closely at the line plots, it is perceivable that all six plots show the stock networks and configuration model networks having the same trend and structure.

Global Clustering Coefficient (Global CC)

Table 17. [Global clustering coefficient values for each of the three configuration model networks]

	Global CC
Pre	0.208
During	0.547
Post	0.227

Although the configuration model networks' global CC values are lower than those of the stock networks, they are still able to capture the sudden increase of clustering magnitude in the during COVID-19 period (more than double the pre and post periods), which can be seen in the stock networks. It can therefore be inferred that the degree of the stock networks is one of the principal

influence on other values and metrics that can be computed from the network, such as betweenness centrality, eigenvector centrality and global CC values. Based on the findings, it doesn't seem like there are many outliers in the networks. Nonetheless, if further analysis is carried out to study the configuration model, one may gather deeper insights such as certain outliers that could be present in the stock networks.

Comparison Between Different Types of Networks

Table 18. [Comparisons between different types of networks in terms of degree distribution, global CC and average path length]

Measure	Period	Real Network	Random Network	Watts-Strogatz Network	Barabasi-Albert Network	Configuration Model Network
Degree Distribution	Pre	Power Law	Binomial	Binomial	Power Law	
	During	Power Law	Binomial	Binomial	Power Law	
	Post	Power Law	Binomial	Binomial	Power Law	
Global Clustering Coefficient	Pre	0.307	0.108	0.373	0.327	0.208
	During	0.621	0.116	0.361	0.339	0.547
	Post	0.315	0.106	0.377	0.302	0.227
Average Path Length	Pre	2.167	2.021	2.216	1.795	
	During	2.132	1.959	2.211	1.781	
	Post	2.261	2.055	2.327	1.822	

From the same data of stocks in the Consumer Products and Services sector, comparisons have been made between real networks, random networks, WS networks, BA networks and configuration model networks in the pre, during and post-COVID-19 periods. Similarity and differences in the structure of these networks have been identified by quantifying their degree distribution, global CC and average path length. These values are listed out in Table 18 as a summary to wrap up the findings.

As can be seen through Table 18, the real networks and BA networks follow a power law distribution whereas the random networks and WS networks follow a binomial distribution. This

comes to show that the financial stock network of Bursa Malaysia is a scale free network. Hubs or vertices with high degree are seen more frequently in these scale free networks as compared to random or WS networks. Thus, all the small degree vertices, or in this case stocks, seem to co-exist with stocks that have many connections (hubs) in the stock network. However, the stocks that get disconnected in the during crisis period do not have any connections to these hubs and in no way can they reach these hubs through any path. Anyhow, as the economy and stock markets begin to recover after the pandemic, the disconnected stocks start to form edges and once again join the giant component, enabling the influence of their neighbours to affect their performance, either positively or negatively.

The global CC values of the stock networks are similar to those of the WS and BA networks, but they still do not capture the sudden increase of the during period's global CC value to 0.621. This could mean that the pandemic has really brought unexpected and drastic changes to the structure of the Malaysian stock market to a point that the predictions of these other simulated networks in the during COVID-19 period are way off. The configuration model however, captures the drastic increase of global CC value in the during period, deeming the degree of the stock networks as a major influence on the structure and pattern of the networks.

The average path length of the real, random and WS networks display similarities in terms of the magnitude of their values. Only the BA networks show lower average path length values than the others as it grows slower than $ln\ N$. It would especially be more obvious in larger networks.

Conclusion

Through this report, threshold networks have clearly shown that the unpredictable conditions caused by COVID-19 have diffused shock and caused a huge change to the structure of the stock network. Positive correlations between stocks increase during COVID-19 besides higher density and clustering tendencies due to the herd behaviour being exhibited. MSTs on the other hand display the hubs of each period and portray that the Consumer Products and Services' stocks do not seem to cluster according to subsector. The centrality measures also reveal that hubs consistently change in rank, but there are certain stocks that constantly appear in the top 5 centrality values. Therefore, market participants cannot simply assume that the Malaysian stock market

behaves similarly all the time, especially during a major event. Extraordinary events tend to cause co-movement of stocks in a homogenous direction, thus reducing the possibility of portfolio diversification. It could be a big hassle for investors who intend to hedge. Concludingly, the results of this report could be beneficial to government officials and market participants in assessing and managing the Malaysian stock market during periods of crisis to make wiser decisions. Extra attention must be given to the hubs of a network as well since they can make or break a market.

Real networks generated using the Consumer Products and Services' stocks seem to exhibit small-world network properties of high clustering coefficient values and low average distance. This is especially more obvious in the network of the during COVID-19 period. In times of chaos, the stocks tend to cluster more closely together, introducing synchronicity where movements of stock prices go in the same direction. Besides that, lower average distance portrays a much quicker and higher efficiency for the spread of positive or even negative effects in the network. Bad impacts caused by the pandemic could easily be passed on from one stock to another, introducing systemic risk. Additionally, the configuration model does a good job in predicting the betweenness and eigenvector centrality structure of the vertices in the stock networks besides giving almost similar global clustering coefficient values. Since the configuration model networks are generated on the basis of the degree sequence of the stock networks, it can be concluded that the degree of the vertices in the stock networks are an important factor in shaping the structure and measurement values of the networks.

References

Bahaludin, H., Abdullah, M. H., Siew, L. W. & Hoe, L. W. 2019. The Investigation on the Impact of Financial Crisis on Bursa Malaysia Using Minimal Spanning Tree. *Mathematics and Statistics* 7(4): 1–8.

Fisher, R. A. 1934. Statistical Methods for Research Workers.

Khoojine, A. S. & Han, D. 2019. Network Analysis of the Chinese Stock Market during the Turbulence of 2015–2016 Using Log-Returns, Volumes and Mutual Information. *Physica A: Statistical Mechanics and Its Applications* 523: 1091–1109.

Kruskal, J. B. 1956. On the Shortest Spanning Subtree of a Graph and the Traveling Salesman Problem. *Proceedings of the American Mathematical Society* 7(1): 48.

Kumar, S., Kumar, S., Kumar, U., Kumar, S., Kumar, P. & Verma, N. 2022. Analysis of Correlation Based Threshold Networks of Dow Jones Stocks of USA: An Econophysics Approach. *Journal of Engineering Science and Technology Review* 15(2): 198–207.

Lai, Y. & Hu, Y. 2021. A Study of Systemic Risk of Global Stock Markets under COVID-19 Based on Complex Financial Networks. *Physica A: Statistical Mechanics and Its Applications* 566.

Luke, D. A. 2015. UseR ! A User's Guide to Network Analysis in R.

Luo, H. 2022. Banking Systemic Risk Estimating of China's Banking Industry during the COVID-19 Pandemic—Based on Complex Network Theory. *Heliyon* 8(11): 11391.

Mantegna, R. N. 1999. Hierarchical Structure in Financial Markets, *Eur. Phys. J. B*.

Memon, B. A. 2022. Analysing Network Structures and Dynamics of the Pakistan Stock Market across the Uncertain Time of Global Pandemic (Covid-19). *Economic Journal of Emerging Markets* 85–100.

Sandoval, L. & Franca, I. D. P. 2012. Correlation of Financial Markets in Times of Crisis. *Physica A: Statistical Mechanics and Its Applications* 391(1-2): 187–208.

Silver, N. C. & Dunlap, W. P. 1987. Averaging Correlation Coefficients: Should Fisher's z Transformation Be Used?, *Journal of Applied Psychology* 72: 146-148.

So, M. K. P., Chu, A. M. Y. & Chan, T. W. C. 2021. Impacts of the COVID-19 Pandemic on Financial Market Connectedness. *Finance Research Letters* 38.

Watts, D. J. & Strogatz, S. H. 1998. Collective Dynamics of "Small-World" Networks. *Nature* 393.

Xia, L., You, D., Jiang, X. & Guo, Q. 2018. Comparison between Global Financial Crisis and Local Stock Disaster on Top of Chinese Stock Network. *Physica A: Statistical Mechanics and Its Applications* 490: 222–230.

Yee, L. S., Mohd Salleh, R. & Mohd Asrah, N. 2018. Multidimensional Minimal Spanning Tree: The Bursa Malaysia. *Journal of Science and Technology* 10(2).